Netherlands Journal of Geosciences — Geologie en Mijnbouw | 84 – 1 | 3 - 24 | 2005

Effects of a Cretaceous structural inversion and a postulated high heat flow event on petroleum system of the western Lower Saxony Basin and the charge history of the Apeldorn gas field

J. Kus[1,2], B. Cramer[1] & F. Kockel[1,3]

1 Bundesanstalt für Geowissenschaften und Rohstoffe (BGR), Alfred-Bentz-Haus, Stilleweg 2, D-30655 Hannover, Germany

2 Corresponding author; email: J.Kus@bgr.de

3 Present address: Eiermarkt 12 B, D – 30938 Burgwedel

Manuscript received: June 2004; accepted: February 2005

Abstract

Thermal history and evolution of the Palaeozoic petroleum system of the western Lower Saxony Basin as well as charge history of the Apeldorn gas field was reconstructed using 2-D forward basin modelling software. The Apeldorn gas field is located on an inverted western rim of the Lower Saxony Basin (LSB) and belongs with its relatively anomalous nitrogen content of 73.9 vol. % to one of the most unique gas accumulations in North Germany. Based on thermal calibration studies utilising both, vitrinite reflectance and corrected bottom hole temperatures as calibration parameters, a shallow burial model and an anomalous event of Coniacian high heat flow of 80 to 120 mW/m^2 was derived. As result, Lower Triassic and younger successions became subjected to slight changes in thermal maturity as opposed to Carboniferous and Permian successions, which show no assessable impact of the high heat flow event on the coalification pattern. The deep burial model in contrary to the shallow burial model is not supported by the structural reconstruction and backstripping in this more marginal setting. According to the modelling results, the key charge of the present Apeldorn gas field began in Tithonian (late Upper Jurassic) during the major phase of rifting in the Lower Saxony Basin. The present Westphalian coal-derived gas accumulations of the Lower Triassic Buntsandstein reservoir were sourced directly from modelled methane pools at top Rotliegend level. The hydrocarbon potential of the Westphalian source rocks became exhausted in Oxfordian (early Upper Jurassic). Reduction of the hydrostatic pressure during the Coniacian high heat flow event together with uplift during the Coniacian-Santonian inversion led to an extensive free gas exsolution. The resulting gas mixture between the exsolved free gas and the Westphalian coal-derived gas reached and saturated Buntsandstein reservoir. The structural trap became destroyed in course of the inversion leading to a sharp decrease of methane and nitrogen saturation.

Keywords: basin modelling; burial; Lower Saxony basin, natural gas; nitrogen, Upper Cretaceous intrusion; vitrinite reflectance

Introduction

The study area with the gas field Apeldorn is located in the Emsland region, NW Germany, on the inverted western rim of the Lower Saxony Basin (LSB) (Fig. 1). LSB is a mature hydrocarbon-producing basin in northern Germany. Within the framework of extensive exploration studies undertaken in the LSB, a deep Palaeozoic gas prone system and a younger, Mesozoic oil prone system were established. The Apeldorn's gas reservoir is of Palaeozoic age. It is located in the Lower Triassic (Middle Buntsandstein) successions and its hydrocarbon components are mainly sourced from Westphalian (Kockel et al., 1994). As a particular feature, the Apeldorn gas field contains 73.9% of nitrogen (Table 1).

The Upper Cretaceous (Santonian-Coniacian) inversion was one of the decisive stages of structural reconfiguration in the LSB, as it played a fundamental role in the hydrocarbon prospectivity of northern Germany. Only a small fraction of the original oil potential, i.e., 6% of the entire potential in the LSB is preserved in reservoirs today and can be produced (Kockel et al., 1994). Moreover, with respect to gaseous HC accumulations in the North German Basin, about 60% of the

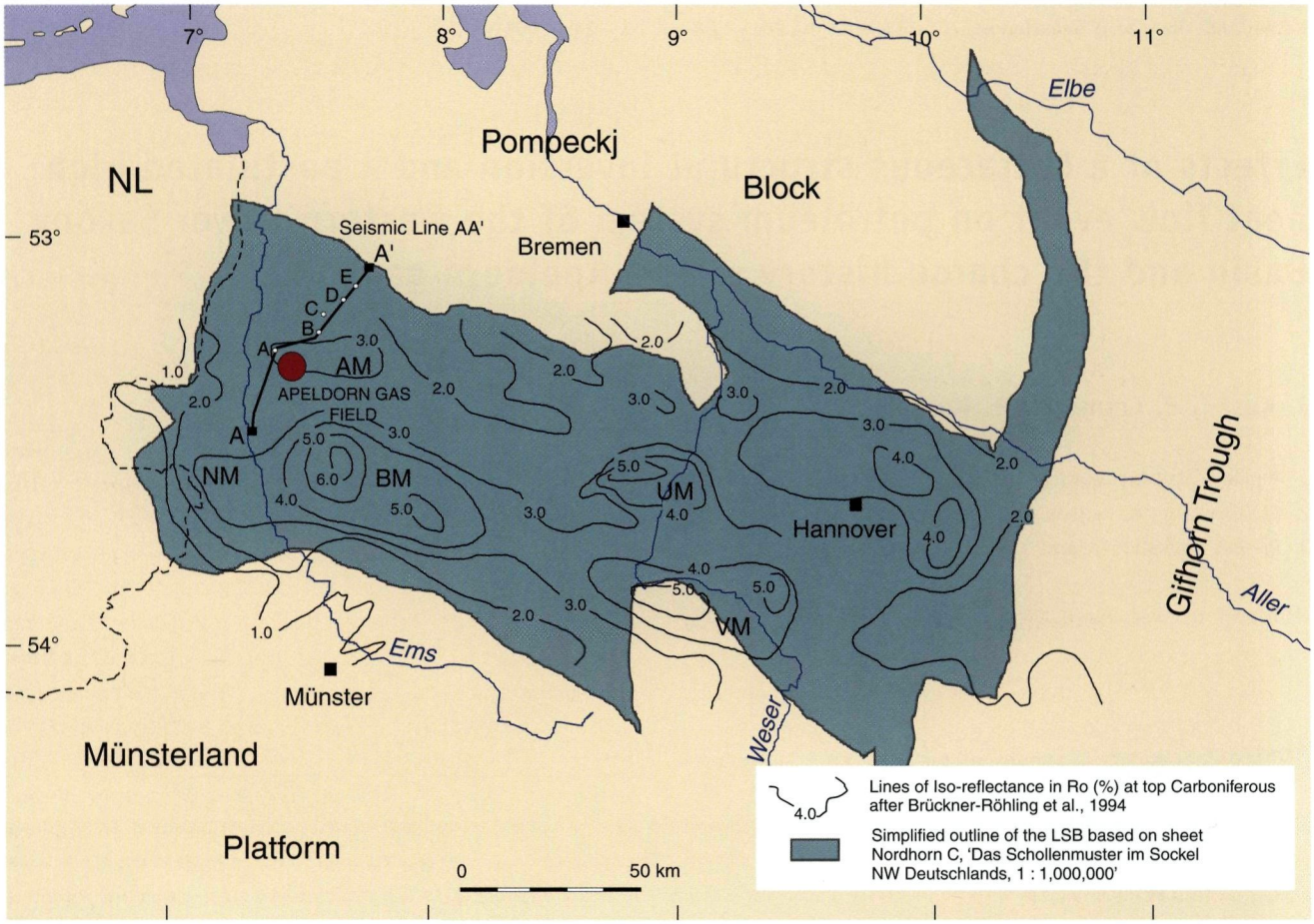

Fig. 1. Location of the study area marked by the seismic line AA' in Emsland region, Western Germany, together with the extent of the Lower Saxony Basin (modified after Baldschuhn, 1996) and the geographic extent of the Middle-Upper Cretaceous Massifs with the associated high maturity areas as indicated by the lines of isoreflectance at top pre-Permian basement. BM-Bramsche Massif, VM-Vlotho Massif, NM-Nordhorn Massif, AM-Apeldorn Massif, UM-Uchte Massif; wells used for calibration: A-Apeldorn, B-Lahner Heide 1, C-Lahn Z1, D-Börger 12 and E-Vrees 1.

German gas deposits of the gas-prone system are situated in basement structures affected by the Late Cretaceous inversion, re-structuring and uplift (Binot et al., 1993; Kockel et al., 1994; Baldschuhn, 1996, et al., 2001; Kockel, 2002).

The existence of Cretaceous intrusives of the LSB: the Bramsche, Vlotho, Uchte, Nordhorn and Apeldorn (Fig. 1) is argued for based on magnetics (Reich, 1933; Hahn et al., 1971), gravity (Plaumann 1983, 1991; Bachmann & Grosse, 1989; Hermes, 1986; Giebler-Degro, 1986; Giebler-Degro et al., 1986) and refraction seismics (Nodop, 1971 and Thyssen et al., 1971).

The Cretaceous intrusives are inferred to be indicative of anomalously high maturity areas and are supposed to have thermally influenced the Palaeozoic gas prone system (Kockel et al., 1994; Leischner, 1994; Düppenbecker, 1991). The Apeldorn intrusive off-shoot body is argued to occur in the study area and to be genetically related to the above Cretaceous plutonic intrusions (Teichmüller et al. 1984; Teichmüller & Teichmüller 1985, 1971; Stadler & Teichmüller 1971; Buntebarth & Teichmüller, 1979; Tischendorf, 1987; Büchner & Seraphim, 1977; Stadler, 1971; Patniak & Füchtbauer, 1975; Schmitz, 1990; Schmitz et al. 1991).

In addition to the Cretaceous intrusive bodies as causes of high maturity, models of high sedimentary burial are also inferred to account for the differentiated high maturity pattern in the LSB (Petmecky et al., 1999; Senglaub et al., 2004; Brink, 2001).

In the past decade, a number of 2D basin modelling simulation studies were undertaken in order to investigate the

Table 1. Averaged gas content and gas isotopes for gas field Apeldorn.

	CH_4 (vol%)	C_2H_6 (vol%)	C_3H_8 (vol%)	N_2 (vol%)	CO_2 (vol%)	$\delta^{13}C_1$ (‰)	$\delta^{13}C_2$ (‰)	$\delta^{13}C_3$ (‰)	δDC_1 (‰)	$\delta^{15}N$ (‰)
Average	25.2	0.3	0.0	73.9	0.5	−19.5	−24.5	−30.0	−123.7	−0.9
Standard deviation	0.1	0.01	0.01	0.09	0.01	0.06	0.06	0.10	1.8	0.21

https://doi.org/10.1017/S0016774600022873 Published online by Cambridge University Press

thermal influence of the Cretaceous intrusives on the basin evolution and on the petroleum systems in the North and/or East German Basin (Graßmann et al., 2003; Friberg, 2001; Petmecky et al., 1999; Büker et al., 1996; Leischner, 1994; Düppenbecker, 1991; Littke et al., 1990).

The objective of this contribution is to investigate not only the thermal influence of one of the postulated Cretaceous intrusives, i.e., the Apeldorn intrusive off-shoot body but far more the effect of the Upper Cretaceous inversion on the Palaeozoic gas prone system in the Emsland area.

The advantages of the chosen area of Apeldorn in comparison with those described and modelled by the previous authors are as follows:

1. The thermal anomaly of Apeldorn is well defined by geophysical means and its influence on hydrocarbon generation potential is local.
2. Gas isotope measurements are available from the Apeldorn Z2 well and represent an additional data set for the purpose of confirmation the resulting assumptions derived from this modelling study calibrated by means of vitrinite reflectance and subsidence history.
3. The geographical location of the Apeldorn anomaly is marginal with respect to the centre of the basinal subsidence and the structural inversion (Ibbenbüren) giving rise to preservation of younger sediments and thus more reliable subsidence model.

The task is undertaken by means of 2D numerical basin modelling simulation performed with the program PetroMod (V.5). In order to achieve this goal, all available vitrinite reflectance data for wells along the cross-section AA' together with surface and bottom hole temperatures (BHT) were utilised in the thermal calibration studies.

Geological setting

The Lower Saxony Basin is a 300 km long and 65 km wide Early Jurassic to Late Cretaceous trough, (see Fig. 1). It forms a string of W-E striking, Late Jurassic – Early Cretaceous rift basins, bounded to the north by the stable Pompeckj Block and to the south by the stable Münsterland platform. To the east, the LSB is limited by the N-S trending Gifhorn Trough and to the west by the Friesland Platform (TNO-NITG, 2001). Sediments attain thicknesses of up to 7500 m. The LSB is superimposed on the folded Late Carboniferous Variscan foredeep and the frontal structures of the Variscan fold belt (Betz et al., 1987). The sedimentary cover of the Caledonian crystalline basement is probably of Lower to Early Middle Devonian age. It is suggested to represent conglomeratic-terrestrial facies of 'Old Red'. Late Middle and Upper Devonian are probably represented by a carbonate platform. The Dinantian – Lower Namurian complex of the Black Shales (Kulm) forms a plastic detachment of low resistance detected by magneto-telluric soundings at a depth of about 7 km (Hoffmann et al., 1995, 1996, 1998). On this detachment, Namurian and Westphalian sequences have been sheered off and intensely folded over the nearly horizontally lying Devonian limestone platform (Franke et al., 1995, 1996).

Overlying the detachment horizon, the higher Namurian sediments (upper A and B) correspond to flysch facies, the Namurian C and the Westphalian A-C to molasse facies with intercalated coal seams and several marine ingressions. In The Netherlands, the thickness of the entire unfolded Namurian amounts to 2000 m. In the non-folded areas in the northwest of the LSB, it amounts to a maximum of about 2000 m (Drozdzewski, 1992; Kockel, 1998).

The coal seams of the Westphalian A-C represent the most important source rock horizon for the Late Palaeozoic petroleum system in NW Germany (Table 2). In the LSB embracing the study area, the thickness of Westphalian B ranges between 700 and 830 m whereas Westphalian C amounts to 750 - >800 m.

The Variscan Orogeny took place in the middle or the end of Westphalian D, which affected also some parts of the basement beneath the LSB (Gerling et al., 1999). Partially preserved volcanic and sedimentary Rotliegend successions attain a thickness of around 100 m in these southern parts of the Rotliegend basin. The first deep-rooted fractures in the pre-Zechstein basin originated in Rotliegend times and again during the Werra cycle of the Zechstein time. During the Zechstein, the successions were characterised by relatively thin shelf and lagoonal deposits of Zechstein 1 and 2 and thin salt deposits of the Zechstein 2-5 (Strohmenger et al., 1996). In the Zechstein and during the Lower Triassic a number of NNE-SSW, trending swells and basins developed in the western LSB, controlling the sedimentation pattern (from W to E: East Netherland swell, Ems trough, Hunte swell). The first rifting processes predated the deposition of the Solling Formation ('H'-unconformity) and gave rise to WNW-ESE-trending lineaments like the Osning lineament and the South Lower Saxony lineament. This evolution continued during the Middle and Upper Triassic. Within the Middle Buntsandstein epoch the Solling Fm., Hardegsen Fm., Detfurth Fm. and the Volpriehausen Fm. contain main reservoir horizons of the Apeldorn gas field. The reservoir sandstones were deposited in a mainly brackish-lacustrine environment under a week marine influence. In addition, there is also an indication for an aeolian or a fluvial influence of the depositional environment. A further intense rifting pulse took place in Middle Keuper times (Lower and Upper Gips-Keuper) preceding the 'Steinmergelkeuper' disconformity. This rifting pulse initiated the generation of many of the Permian salt diapirs in NW-Germany. With the beginning of the Liassic, the LSB began to form in a dilatational stress field. The sedimentation in the LSB was governed by horsts and swells as well as grabens and elongated basins, mainly trending WNW-ESE (Kockel et al., 1999). Late Toarcian Posidonia Shale is a principal source rock in the Mesozoic petroleum systems (Schmitz 1968). The extension of the rift basin reached its

https://doi.org/10.1017/S0016774600022873 Published online by Cambridge University Press

Table 2. Source and reservoir rocks, seals and HC generation in the Northwest German oil and gas provinces (Kockel & Franzke, 1998); source and reservoir rocks marked in red were incorporated into the modelling study.

Time	Source rocks	Principle reservoir rocks	Seals	Formation of principle traps	HC generation
Tertiary			Palaeogene clays	⇐ halokinesis	second generation of oil at the fringes of the basin
Maastrichtian		calcarenites (Reitbrook)			
Campanian		sdst. (Steinförde)			
Coniacian- Santonian				⇐ inversion: (detached anticlines, rollover structures in overburden, salt intrusions) (horsts, half-horsts in Permian)	generation of oil + condensates near Cretaceous plutons
Barremian to Albian			Lower Cretaceous claystones	⇐ discordancy traps	first generation of oil from Liassic + Berriasian source rocks in basin centre
Hauterivian		Gildehaus sdst.		⇐ discordancy traps	
Valanginian		*Dichotomites* sdst. Bentheim sdst.		⇐ facies traps ⇐ rifting, block-faulting, halokinesis	
Berriasian	limnic bituminous 'Blätterschiefer' ('Wealden') (I)	lumachelle limestone, deltaic sdst. ('Wealden')		⇐ rifting, block-faulting	
Upper Jurassic		Aldorf *Serpula* limestone (Portlandian), dolomitic limestones (Eimbeckhausen, *gigas*, Kimmeridgian), sdst. (Kimmeridgian) oolithic limestone (Oxfordian)	halite (Münder Mergel) (Portlandian)	⇐ rifting, block-faulting, halokinesis ⇐ rifting, block-faulting, halokinesis	
Middle Jurassic		deltaic sdst.:*ornata* sdst. + *macrocephalus* sdst. (Callovian) *aspidoides* sdst, *württembergica* sdst. (Bathonian) *garantiana* sdst. (Bajocian), near-shore sands: *coronata* + *sonnina* sdst. (L. Bajocian), *concava*, *obtusa*, *staufensis* + *sinon* sdst. (Aalenian)		⇐ *rifting*, block-faulting, halokinesis ⇐ facies traps	
Liassic	*Posidonia* shale in Lower Toarcian (II/III)	coastal sdst. (Hettangian)			second generation of gas from Carboniferous coals by re-coalification
Keuper		deltaic sdst. (Rhetian)	halite (Middle Keuper)	⇐ rifting, halokinesis	
Muschelkalk			halite (Middle Muschelkalk)		
Buntsandstein		sdst. in Solling, Detfurth + Volpriehausen	halite (Upper Buntsandstein)	⇐ rifting, halokinesis	
Zechstein 4-7 Leine cycle Staßfurt cycle Werra cycle	Stinkschiefer (zCa2) (II) [Copper shale (zT1) (I/II)]	Plattendolomite (zCa3) Hauptdolomite (zCa2)	halite (Zechstein 2-7)		
Rotliegend		aeolian, fluviatile and beach sdst. in Upper Rotliegend	halite (Upper Rotliegend)	⇐ rifting	
Westphalian	Coal seams (Westphalian C) (III) Coal seams (Westphalian A+B) (III)	fluviatile sdst. in Westphalian A-C		⇐ Variscan folding	first generation of gas from Carboniferous coals by subsidence of the Molasse trough
Namurian	Coal seams (Namurian C) (III) dispersed plant material in distal Flysch (III) (Namurian A-B), bituminous black shales (Namurian A) (II)	Deltaic and fluviatile sdst. in Namurian C			
Dinantian	bituminous black shales (II)*				

* I, II, III = kerogen types

https://doi.org/10.1017/S0016774600022873 Published online by Cambridge University Press

peak during the Portlandian, when the basin was totally cut off from the open ocean (Gramann et al., 1997), and stopped in most parts of the LSB during the Middle Aptian. The lowermost Cretaceous sediment Berriasian, or the 'Wealden' = Bückeburg Fm.) are brackish to limnic in facies and contain high amounts of sedimentary organic matter with good hydrocarbon potential. These rocks act as petroleum source rocks some Cretaceous reservoir rocks in the studied area like it is the case with the marine Bentheimer sandstone of Valanginian age (Boigk, 1981; Wonham et al., 1997). In the centre of the LSB a number of Cretaceous plutonic intrusions like the Bramsche, Vlotho, Uchte, Nordhorn and Apeldorn are argued to account for the anomalous coalification values in the Carboniferous (Teichmüller & Teichmüller, 1950, 1951; Stadler & Teichmüller, 1971; Buntebarth & Teichmüller, 1979; Bartenstein et al., 1971; Koch & Arnemann, 1975; Deutloff et al., 1980) as shown in Fig. 1. The lines of iso-reflectance in Fig. 1 are based on the overall number of 230 measurements carried out at the Top Carboniferous surface. Numerous thermal, geochemical, geophysical (magnetic and gravity anomalies) and geological indicators are in favour of the postulated emplacement and its thermal influence of the overburden in NW Germany (Reich, 1933; Teichmüller & Teichmüller, 1950, 1951; Schreyer, 1968; Schreyer, 1969; Bartenstein et al., 1971; Fabian, 1971; Hahn et al., 1971; Nodop, 1971; Stadler & Teichmüller, 1971; Thyssen et al., 1971; Koch & Arnemann, 1975; Patniak & Füchtbauer, 1975; Büchner & Seraphim, 1977; Buntebarth & Teichmüller, 1979; Teichmüller et al., 1979; Deutloff et al., 1980; Stadler & Teichmüller, 1982; Plaumann, 1983; Brauckmann, 1984; Giebler-Degro, 1986; Giebler-Degro et al., 1986; Hermes, 1986; Richter et al., 1986; Tischendorf, 1987; Bachmann & Grosse, 1989; Plaumann, 1991).

With the beginning of the Coniacian, a structural inversion took place in the LSB (Baldschuhn et al., 1985; Baldschuhn et al., 1991; Baldschuhn & Kockel, 1994; Baldschuhn, 1996; Kockel, 2002). The sedimentary fill of the former basins or grabens became pushed onto its flanks or shoulders. Former normal border faults were transformed into reverse faults or thrusts or into 'phaeno-normal faults'. Zechstein salt may have acted as a lubricant along these thrusts at the level of the Upper Buntsandstein Röt Formation (Baldschuhn et al., 1998). Contemporaneously, rapidly subsiding 'subsequent marginal troughs' (Voigt, 1962a) sank into the former graben or basin shoulders, which are often filled with partly turbiditic sediments or even olisthostromes (Voigt, 1962b). This stage ended in the LSB in the Campanian. The amount of uplift is estimated to 400 - 500 m in the studied area, but up to 8000 m in the Ibbenbüren region (Baldschuhn & Kockel, 1999). In a next stage a non-ruptural and flexure-like uplift of the individual inversion structures or the inverted basin as a whole continued and ended in Maastrichtian. In a last stage (Late Palaeocene to Miocene), 'relaxation' movements can be observed along some of the compressional reverse faults.

Gas Field Apeldorn

First examinations of reflection seismic profiles acquired in 1949 over the Apeldorn area revealed a broad and gentle anticline striking E-W in the upper part of the Mesozoic overburden (Fig. 2). The target of the first exploration wells was the petroleum-geological relation between the Wealden and Valanginian (Valendis) sandstone. The production tests on the oil impregnated Wealden and Apt failed to prove commercial accumulation of gas. The oil impregnation at Wealden and Apt level originates most probably from the access to a deep Wealden kitchen located outside the section. In 1964, Preussag GmbH announced the discovery of a Middle Buntsandstein gas field at Apeldorn. The exploration well Apeldorn

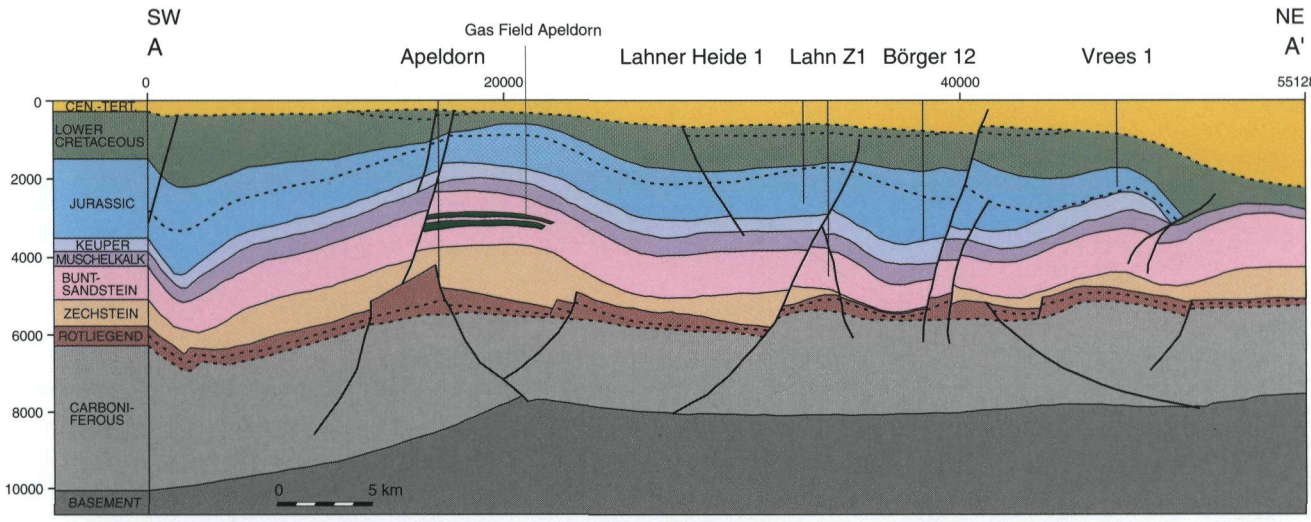

Fig. 2. A geological cross-section AA' displaying location of the gas field Apeldorn and calibration wells of Apeldorn, Lahner Heide 1, Lahn Z1 and Börger 12. Dotted lines indicate unconformities. The vertical scale is exaggerated by 25% (Cross-section: Cenozoic-Top Stephanian after Wehner et al., 1989 and Top Stephanian-Top Basement after Kockel, 1998; Drozdzewski, 1992).

https://doi.org/10.1017/S0016774600022873 Published online by Cambridge University Press

Table 3. Random vitrinite reflectance (Rr %) measurements utilized for the calibration of the thermal evolution of the Palaeozoic, Mesozoic and Cenozoic sedimentary units along the seismic section AA'.

	X Coordinates	Y Coordinates	Depth below sea level in m	Random Vitrinite Reflectance Rr %	Number of Measured Vitrinite	St. Deviation %
Lahn Z1	3406275	5853865	96	0.25	40	0.03
Lahn Z1	3406275	5853865	391	0.33	9	0.02
Lahn Z1	3406275	5853865	651	0.35	42	0.04
Lahn Z1	3406275	5853865	931	0.36	7	0.03
Lahn Z1	3406275	5853865	1502	0.47	35	0.07
Lahn Z1	3406275	5853865	1906	0.60	10	0.06
Lahn Z1	3406275	5853865	2376	0.73	12	0.07
Lahn Z1	3406275	5853865	2631	1.20	45	0.14
Lahn Z1	3406275	5853865	4234	3.86	11	0.36
Lahn Z1	3406275	5853865	4236	2.85	11	0.45
Lahn Z1	3406275	5853865	4238	3.06	32	NA
Lahn Z1	3406275	5853865	4245	2.38	62	0.22
Lahn Z1	3406275	5853865	4248	2.57	30	0.076
Lahn Z1	3406275	5853865	4352	3.48	6	0.43
Lahn Z1	3406275	5853865	4378	3.38	20	0.43
Lahner Heide 1	3404050	5855365	1297	0.50	NA	NA
Lahner Heide 1	3404050	5855365	1303	0.51	NA	NA
Lahner Heide 1	3404050	5855365	1372	0.55	NA	NA
Lahner Heide 1	3404050	5855365	1407	0.59	NA	NA
Lahner Heide 1	3404050	5855365	1465	0.69	NA	NA
Lahner Heide 1	3404050	5855365	1472	0.70	NA	NA
Lahner Heide 1	3404050	5855365	1524	0.71	NA	NA
Lahner Heide 1	3404050	5855365	1581	0.74	NA	NA
Lahner Heide 1	3404050	5855365	1647	0.81	NA	NA
Lahner Heide 1	3404050	5855365	1712	0.87	NA	NA
Lahner Heide 1	3404050	5855365	1826	0.88	NA	NA
Lahner Heide 1	3404050	5855365	1885	0.82	NA	NA
Lahner Heide 1	3404050	5855365	1893	0.85	NA	NA
Lahner Heide 1	3404050	5855365	1902	0.87	NA	NA
Apeldorn 7	2592115	5848130	164	0.23	13	0.05
Apeldorn 7	2592115	5848130	224	0.25	12	0.05
Apeldorn Z3	2592030	5845800	3624	2.86	9	0.25
Apeldorn Z3	2592030	5845800	3729	2.41	NA	NA
Apeldorn Z2	2593265	5845595	4016	3.01	NA	NA
Apeldorn Z2	2593265	5845595	4040	2.71	4	NA
Apeldorn Z2	2593265	5845595	4111	2.53	4	0.32
Apeldorn Z2	2593265	5845595	4115	2.12	12	0.32
Apeldorn Z2	2593265	5845595	4132	3.18	11	NA
Apeldorn 10	2594225	5850315	308	0.28	6	0.1
Apeldorn 10	2594225	5850315	523	0.33	4	0.06
Apeldorn 10	2594225	5850315	918	0.51	2	0.08
Apeldorn 10	2594225	5850315	803	0.41	3	0.04
Börger 12	3408735	5858170	1830	0.62	18	0.059
Börger 12	3408735	5858170	2174	0.76	50	0.08
Börger 12	3408735	5858170	2176	0.70	50	0.047
Vrees 1	3415340	5864067	1963	0.40	18	0.07

T1 intersected a gas column in the Lower Triassic Buntsandstein over the interval 2227.5 to 2509.5 m. The exploration well Apeldorn T1 reached a total depth of 2542 m and was suspended as a gas producer. The gas of the Apeldorn field is trapped to the west by a fault trap and to the east, south and north by the dipping flanks of the Apeldorn anticlinal structure (Boigk 1952). The gas-bearing trap has up to 30 m of net reservoir with an average porosity in the range between 10 and 16.5%. The cumulative production – in 2002 – amounted to 4.27 $G \cdot m^3$ (Vn) (Pasternak et al., 2003).

The gas from the Apeldorn field is dominated by a high nitrogen content of 73.9 vol. % with a stable isotope signature ($\delta^{15}N$) of –0.9‰ (Gerling et al., 1995). With 25.2 vol. % methane is the most abundant hydrocarbon component. According to empirical maturity relationships (e.g., Faber, 1987), the stable carbon isotope ratio of methane coincides with a thermal gas generation from a terrestrial source rock at a high level of maturation (above 2% Rr). The most probable sources of methane are the coal measures in the Westphalian. About 0.4 vol. % of the gas at Apeldorn consists of hydrocarbons other than methane, which corresponds to about 1.7 vol. % of the hydrocarbon fraction (Table 1).

Methods

Organic Petrography

Random vitrinite reflectance measurements (Rr %) were performed according to the International Standard (ISO7404 1984 part 5), (Table 3). Detailed measurements were carried out on whole rock or crushed samples under standardised conditions (immersion oils with a refractive index of 1.518, wave length of 546 nm, Leica MPV2 photometer microscope, objective lens 50 ×, eyepieces 10 ×).

Basin modelling

The numerical modelling software PetroMod (IES, Jülich) was utilised in calibration of burial and thermal histories as well as in the in reconstruction of the history of Palaeozoic petroleum system.

Measured and modelled (Burnham & Sweeney 1989, Easy%R_0 kinetic model) vitrinite reflectance values provide the most essential information on thermal evolution of source rock maturity during basin subsidence. The match between the measured and modelled values of vitrinite reflectance permits a calibration of the thermal history within the basin. It can be obtained by varying the input parameters such as thickness and erosion rate, thermal conductivity of the sediments, heat flow etc.

The subsidence model is based on a geological conceptual model of the geological history of the study area. It is characterised by a number of geologic events and/or layers defined by absolute time limits and by type of event, i.e., sedimentation, hiatus, erosion. The following input-parameters have to be quantified for each of the events in order to simulate sedimentary basin development processes: present and original thickness, lithologies, present porosities, cementation or fracturing, present and palaeobathymetry, sediment-water interface temperatures, palaeoheat flow, physical and thermal properties of the lithologies, fluids and organic material (for the latter a data base of default values for common material types is given). The reconstruction of the evolution of the petroleum system requires further input parameters such as source and reservoir rocks, TOC values as well as kinetic models for petroleum generation. Source rocks kinetics for methane and nitrogen generation is applied after Krooss & Leythaeuser (1988). Migration modelling methods involve both, the Darcy flow modelling of 3-phase petroleum migration (water, liquid HC, vapour HC) driven by buoyancy, pore and capillary pressures and the diffusion of light hydrocarbons in water. Following an initial decompaction of the section, the processes of deposition, hiatus and erosion are modified forward through time, giving rise to a contemporaneous calculation of pore pressure regime. During simulation, heat flow is not assumed throughout the section, but depends on the thermal conductivities and heat capacities of the rocks.

The model applied considers a basal heat flow as single heat source. In the applied model, basal heat flow is set at the base of the section and is then transported through the sedimentary column by means of conduction to the surface. Surface heat flow can be then calculated at the section's surface.

Lacking both, a detailed control on the timing of fault opening and closure periods as well as values for the respective fault permeablities within the study area, a simple fault model was introduced into the 2D basin modelling study. In the modelling study, fault structures were modelled as high- or as low-permeable zones of migration pathways. These faults are a critical parameter in the applied model as their behaviour during the active phases of structural reconfiguration is a mere assumption. During the compression, the behaviour of faults is referred to as a non-transmittable as opposed to dilatation phases where faults are assumed to be open for vertical and horizontal transmissibility.

Burial history, subsidence, uplift and erosion

Subsidence reconstruction along the profile AA' was established by Wehner et al. (1989) using data sets of 15 wells situated along the transect. The subsidence pattern was interrupted by major and minor phases of non-deposition and/or erosion giving rise to sites of major unconformities and hiati (Wehner et al. 1989), (Table 4). The stratigraphic table of Menning et al. (1997), containing appropriate formation ages and durations, provided the base for the stratigraphic subdivision of the 2D model.

https://doi.org/10.1017/S0016774600022873 Published online by Cambridge University Press

Table 4. Input data for selected wells along the studied seismic section. Negative values give thicknesses of eroded sediments; heat flow values are in mW/m².

Event Name/ No	Event Name	Age (Ma)	Lithology	*Apeldorn*		*Lahner Heide 1*		*Lahn Z1*		*Börger 12*	
				Thickness in m	Heat flow	Thickness in m	Heat flow	Thickness in m	Heat flow	Thickness in m	Heat flow
tmi-q	Miocene-Quaternary	25	Sand&Silt	70	65	153	50	146	65	261	55
tolm-tolo	M-U Oligocene	34	Sand&Silt	0	63	19	63	7	63	67	63
erosion	U Eocene-L Oligocene	36	Sand&Silt	-50	62	0	63	0	62	0	62
teom	M Eocene	42	Sand&Shale	34	62	53	62	90	62	35	62
teou	L Eocene	54	Shaly Lime	130	62	242	62	186	62	251	62
erosion	Danian-L Eocene	59.5	Shaly Lime	-23	61	0	61	0	61	0	61
erosion	Danian-L Eocene	65	Marl	-91	85	-363	70	-350	75	-279	75
krca-krma	Camp-Maastrichtian	84	Marl	120	85	261	75	175	80	279	80
krcc+krsa	Coniacian-Santonian	87	Shaly Lime	196	85	231	110	62	75	31	80
erosion	Coniacian	89	Shaly Lime	-136	85	-52	115	-250	70	-260	85
krc	Coniacian	91	Shaly Lime	130	90	160	140	50	85	60	85
krt	Turonian	94	Marly Lime	166	95	73	69	180	69	200	69
erosion	Albian	97	Shaly Lime	0	69	0	69	0	69	0	69
krl	Albian	112	Shaly Lime	192	68	230	68	170	68	108	68
krh-krp	Valanginian-Aptian	136	Calc Shale	25	65	215	65	207	65	303	65
UV2	Bentheimer Sst	135	Shale	25	65	25	65	29	65	25	65
UV1	Bentheimer Sst	137	Calc Shale	24	65	20	65	22	65	17	65
Wd1-6	Wealden	144	Shale&Sst	113	60	126	60	122	60	221	60
joki-jopo	Kimmerid.-Serpulit	150	Sandy Shale	197	60	94	60	66	60	536	60
erosion	Heersumer Sch.-Korallenoolith	154	Sandy Shale	-160	67	-44	67	-20	67	-53	67
jutco-jm	U Toarcian-Callovian	180	Sandy Shale	311	95	502	95	576	95	570	95
posidon	L Toarcian	189	Sandy Shale	30	95	30	95	29	95	30	95
ju	Hettan.-Pliensbach.	205	Calc Shale	452	95	521	95	450	95	526	95
k	Keuper	231	Evap. Shale	273	67	313	67	300	67	487	67
m	Muschelkalk	240	Shaly Lime	464	62	426	62	418	62	406	62
so	U. Buntsand	244	Salt&Anhy	125	60	125	60	128	60	109	60
sm	M. Buntsand	249	Shale&Sand	363	60	330	60	270	60	246	60
su	L . Buntsand	251	Silty Shale	296	60	358	60	507	60	242	60
26	Aller Salt	252.5	Salt	94	67	26	67	20	67	9	67
25	Red Halite Clay	253	Salt&Slilt	21	67	17	67	18	67	3	67
24	Leine Salt	253.2	Salt	200	67	102	67	25	67	1	67
23	Hauptanhydrite	253.5	Anhy	35	67	31	67	22	67	1	67
22	Straßfurt Salt	254	Salt	124	67	27	67	11	67	3	67
21	Basalanhydrite	255	Anhy	6	67	54	67	22	67	6	67
20	Main Dolomite	255.5	Dolomite	16	67	27	67	11	67	3	67
19	Main Dolomite	256	Dolomite	61	67	27	67	11	67	3	67
18-17	Werra Cycle	257.5	Salt&Anhy	52	67	81	67	33	67	6	67
cushale	Copper Shale	258	Shale	10	70	9	70	9	70	9	70
ro	U Rotliegend	291	Shale&Sand	317	70	56	70	86	70	85	70
erosion	L Rotliegend	290	Tuff.Shale	110	80	0	80	0	80	0	80
ru	L Rotliegend	298	Tuff.Shale	-349	80	-369	80	-370	80	-375	80
cst	Stephanian	305	Silt&Sand	806	90	505	90	591	90	473	90
erosion	Westphalian D	306.5	Sandy Silt	-192	90	-192	90	-192	90	-192	90
cwd	Westphalian D	308	Sandy Silt	461	90	313	90	368	90	261	90
cwc	Westphalian C	311	Sandy Silt	358	75	446	75	428	75	366	75
cwb	Westphalian B	313.5	Sandy Silt	568	75	418	75	430	75	360	75
cwa	Westphalian A	316.5	Sandy Silt	572	75	266	75	280	75	256	75
n	Namurian	326.5	Shale	892	75	1000	75	1024	75	1022	75
1	Basement	400	Basement	3080	75	3053	75	3053	75	3080	75

https://doi.org/10.1017/S0016774600022873 Published online by Cambridge University Press

Present-Day and Sediment-water interface temperatures

A present day annual surface temperature of 8° C together with corrected bottom hole temperatures (BHT) were used to calibrate a present day temperature at the following wells: Apeldorn Z2, Lahner Heide 1, Börger 12, Vrees 1 and the Emsland region, (Fig. 3). On average, three BHT measurements in depths from 209 m to 4307 m were used applying the Horner correction, Explosions-line source correction (Lachenbruch & Brewe, 1959), and Explosions-cylinder source (Leblanc, 1982). As further input data, the sediment-water interface temperatures (SWI) were calculated by the PetroMod software based on palaeo-geographic latitudes, palaeoclimatic data and water depths (IES PetroMod/Reference Manual).

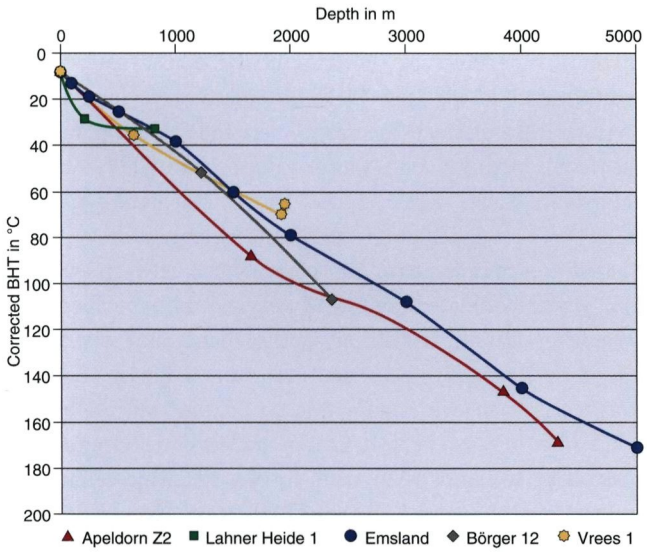

Fig. 3. Corrected BHT obtained for wells Apeldorn Z2, Lahner Heide 1 and Börger 12 and averaged corrected BHT's for the entire Emsland region after Wohlenberg (1979) and Haenel (1980).

Source rocks

In order to reconstruct the evolution of the Palaeozoic petroleum system, source rock units had to be defined. Source rock characteristics required for modelling gas generation comprise initial TOC values, initial generation potentials, and reaction kinetic models for the gas generation.

Upper Carboniferous, i.e., Westphalian A, B and C, represent gas-prone (type III) source rocks favourable of methane and nitrogen generation. The averaged TOC content of this main gas source rock in the study area was estimated to 3% in Westphalian A, to 4% in Westphalian B and to 2.5% in Westphalian C. These estimates are based on a measured proportion of coal seam thicknesses in the Westphalian A, B and C in the Ruhr area (Drozdzewski, 1992). The percentage of coal within the Witten Fm. and Bochum Fm. of Westphalian A amounts to 2 - 2.5% and 5.5 - 6% respectively. On the contrary, Essen Fm. and Horst Fm. of Westphalian B contain 4.5 - 5% and 5 - 6% respectively, whereas Dorsten Fm. and Lembeck Fm. of Westphalian C contains only 2 - 4% and 1 - 4% respectively.

By comparison, Leischner (1994) reports TOC values of 0.43 - 2.66% measured for Upper Carboniferous in Emsland region. Scheidt & Littke (1989) report 2% of TOC content in siliciclastic sedimentary rocks of the Ruhr Basin whereas measured TOC values in coal seams are respectively more than two times higher.

The initial HI values for the above source rock units accountable for methane generation were set to 100 mg/g TOC (Büker, pers.com. 2000). Presently measured HI values for the Upper Carboniferous in the Emsland region are given in the range of 50 mg/g TOC to 5 mg/g TOC and represent exhausted HI values as opposed to initial values (Leischner, 1994). On the contrary, an initial HI for these source rock units accountable for generation of nitrogen gas was set to an estimated value of 20 mg/g TOC, (Büker, pers.com. 2000).

The reaction kinetics for methane and nitrogen generation from Carboniferous coals was applied according to Krooss & Leythaeuser (1993).

Fault seal Model

The modelled sealing capacity along the faults at the Apeldorn gas field plays a critical role in terms of methane and nitrogen accumulation through the geological time. The property of modelled fault sealing and opening was modified throughout the geological history in accordance to the appearance of major structural events seen in Table 4. The main modelled conductive phases were set in Carboniferous-Permian (302 - 284 Ma), Permian-Triassic (251 - 245 Ma), Late Triassic – Jurassic (205 - 112 Ma), Cretaceous (89 - 84 Ma) and Cretaceous – Paleogene (65 Ma). In the simulation software PetroMod (V. 5), the petrophysical properties of the seals are represented exclusively by vertical and horizontal permeability or transmissibility factors ranging from 0 to 1. In this basin modelling study, both, the vertical as well as the horizontal transmissibility factors were set to 1 during main modelled conductive phases, giving rise to gas or/and fluid transmission across the faults. These together with timing of fault activation as a critical parameter allow a quantitative estimation of timing of seal development and seal stability. In nature, the sealing ability depends on the number of the faults within the fault plane, stress field, amount of displacement, and smearing effect of shales along fault and the percentage of clay component in the 'shales' throughout the geological history (Sneider et al. 2000).

Results

2D basin modelling study was conducted to assess the thermal influence of the postulated Coniacian high heat flow event. Furthermore, the effect of the Upper Cretaceous inversion on the charge history of the Apeldorn gas field was assessed.

https://doi.org/10.1017/S0016774600022873 Published online by Cambridge University Press

Heat flow history

In the study area, there is neither a direct evidence of deep burial nor of magmatic events. The most convincing indirect evidence of magmatic intrusion comes from positive gravity and magnetics anomalies (Reich, 1933; Hahn et al., 1971; Plaumann, 1983, 1991; Bachmann & Grosse, 1989; Hermes, 1986; Giebler-Degro, 1986; Giebler-Degro et al., 1986).

Deep burial scenario as opposed to a shallow burial model refers to an enormous amount of sediments being accumulated prior to the Coniacian-Santonian inversion and eroded during the inversion. Deep burial model contradicts the palaeogeographic evolution in the study area. Its application is unequivocally not supported by the reconstruction of the palaeogeographic framework and the tectonic evolution at the margins of the LSB, i.e., along the cross-section AA' (Wehner et al., 1989). The subsidence curves in Figs. 5 and 6 are based on a detailed reconstruction of the tectonic evolution derived from a number of interpreted seismic sections, inclusive the seismic section along the cross-section AA' and numerous bore hole data available in the area. The structural reconstruction and backstripping carried out by Wehner et al. (1989) does not account for an intensive subsidence prior to Coniacian and major phases of erosions during the Coniacian-Santonian inversion in the study area. The accuracy of the reconstructed thicknesses of partially or entirely eroded stratigraphic section ranges between 50 and 150 m. Instead, prior to the Coniacian-Santonian inversion, i.e., at 89 Ma ago, the top of Carboniferous at Lahner Heide 1 well was buried to a relatively shallow depth of only 4000 m compared to a maximal burial depth of 6000 - 8000 m in the vicinity of the anomaly centre at Ibbenbüren (Baldschuhn & Kockel, 1999). Subsequently to the Upper Cretaceous structural inversion, i.e., at 84 Ma, the respective depth of burial of top Carboniferous was reduced by a value of 250 m to the maximum of 400 m of erosion in the north-eastern and south-western part of the cross-section. The above subsidence pattern, together with the erosion episodes along the cross-section AA' speaks in favour of the shallow burial model.

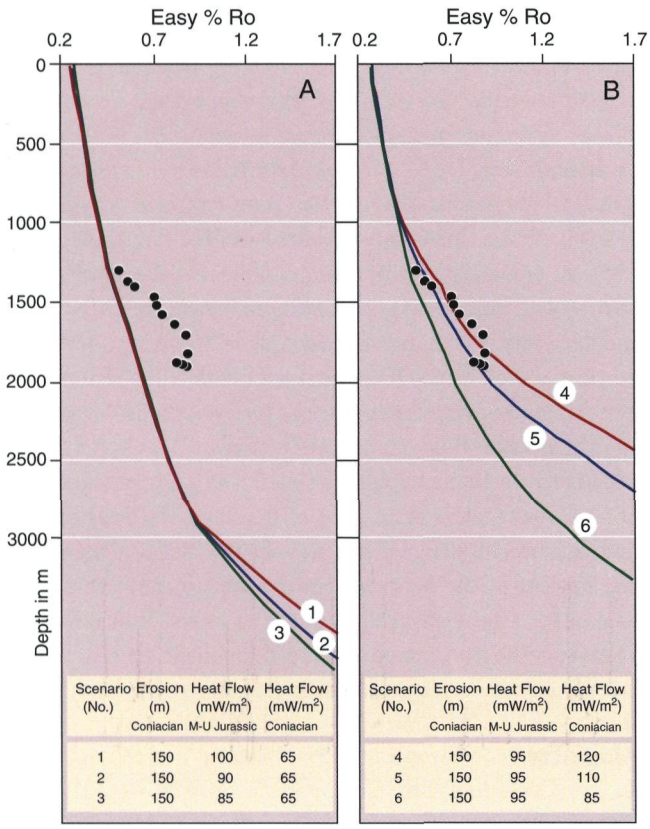

Scenario (No.)	Erosion (m) Coniacian	Heat Flow (mW/m²) M-U Jurassic	Heat Flow (mW/m²) Coniacian
1	150	100	65
2	150	90	65
3	150	85	65

Scenario (No.)	Erosion (m) Coniacian	Heat Flow (mW/m²) M-U Jurassic	Heat Flow (mW/m²) Coniacian
4	150	95	120
5	150	95	110
6	150	95	85

Fig. 4. Shallow burial (A) and heat flow (B) models during the Coniacian at Lahner Heide 1 well. The maturity trend line 4 corresponds to the best-fit scenario of the high heat flow model.

Furthermore, the rejection of the deep burial model is additionally supported by differential burial maps. Wehner et al. (1989) compiled a number of such difference maps for vitrinite reflectance at the Base Liassic in the eastern and western part of the LSB. These difference maps show in the western LSB a distinct discrepancy between the calculated and measured vitrinite reflectance values. Calculated vitrinite reflectance values were computed with a temperature gradient of 33° C/km and with an averaged surface temperature of 15° C. The difference in the absolute values ranged between >1% and 3%, which correlated well with gravimetric anomalies (the Bramscher Massif, Massifs of Vlotho, Uchte und Nordhorn) shown by Plaumann (1983) and Bachmann & Grosse (1989) in gravimetric maps with and without a Bouguer reduction.

In order to test a hypothesis of a shallow burial model, three distinctive scenarios were assed for the following calibration wells: Apeldorn, Lahn Z1, Lahner Heide 1 and Börger 12, (Fig. 4). The assessment involved application of both, the shallow burial ranging from 50 m to 260 m for the above wells during Coniacian & Santonian and differentiated heat flow values during two structural events: the Middle to Upper Jurassic rifting event and the postulated high heat flow event during Cretaceous. During the Middle-Upper Jurassic rifting event, heat flow values were sequentially varied from 85, 90 to 100 mW/m^2, whereas a heat flow of 65 mW/m^2 was left unaltered for the time span of 3,2 Ma during the postulated high heat flow event in the late Middle Cretaceous, i.e. Coniacian. The time span i.e., an assumed high and short termed heat flow event is based on the following: 2 Ma applied during Coniacian in the LSB by Petmecky et al., (1999), ca. 19 Ma applied during Turonian-Campanian in LSB by Düppenbecker (1991), 6 Ma applied during Late Turonian-Santonian in the LSB by Leischner (1994) and to 7.7 Ma during Turonian-Coniacian by Buntebarth (1985).

Fig. 4a displays the application of the three scenarios at Lahner Heide 1 well. Based on the above input parameters, neither of the calculated maturity curves fits the measured vitrinite reflectance data. In summary, it fails to explain the vitrinite reflectance pattern and therefore the observed maturity profile cannot be solely accounted for by the shallow burial model.

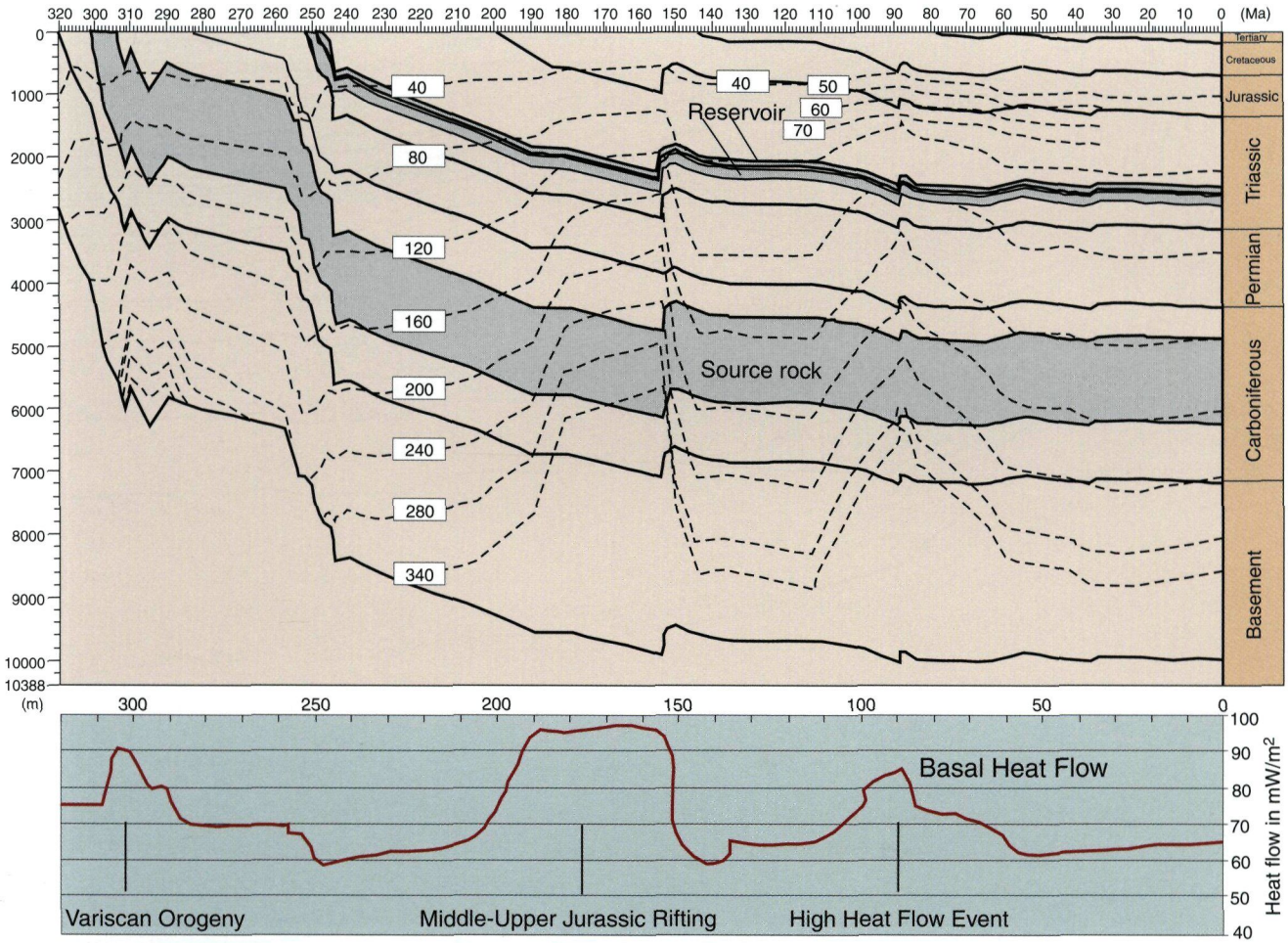

Fig. 5. Burial history diagram, vertical temperature distribution and heat flow history (High heat flow model, scenario 4) at Apeldorn Z2 well.

Given that neither the shallow burial nor the deep burial approach alone satisfy the maturity trend reflected by the measured vitrinite reflectance data as well as the palaeogeographic framework, a high heat flow model was applied with a high heat flow event during Coniacian (Cretaceous) for a time span of 3.2 Ma. In this high heat flow model, a heat flow of 95 mW/m^2 was used for the Lower and Middle Jurassic rifting period whereas during the high heat flow event values ranging from 95 to 120 mW/m^2 were sequentially applied. The erosion values for the period of Coniacian to Santonian remained unaltered (Fig. 4b).

The calculated curve trend of organic matter maturation based on heat flow value of 85 mW/m^2 does not show a good fit with the measured vitrinite reflectance values (scenario 6). The curve (scenario 5) calculated with a higher value of 110 mW/m2 provides a better fit. The trend (scenario 4) calculated with heat flow of 120 mW/m^2 for the Coniacian provides the best match with the measured vitrinite reflectance. This high heat flow scenario can be successively applied in the remaining calibration wells. The resulting heat flow histories for the four calibration wells are listed in Table 4. As shown there, the maximum heat pulses during Coniacian-Santonian differ for the four wells between 120 and 80 mW/m^2.

As a result of the applied Coniacian high heat flow event, a marked change of the temperature and maturity distribution was observed. At Apeldorn Z2, temperature at top Westphalian (source rock) increased well from 180° C shortly prior to the postulated high heat flow event to a temperature of 220° C during the event. A burial history diagram in Fig. 5 depicts calculated thermal evolution at well Apeldorn Z2. Three high heat flow events characterise the thermal evolution at well Apeldorn: the Variscan Orogeny, the Middle to Upper Jurassic rifting event and the postulated high heat flow event in the late Middle Cretaceous.

The most important effect of the modelled Coniacian high heat flow event on maturity distribution is an increase in the calculated vitrinite reflectance values in the Mesozoic and Cenozoic successions during and postdating the event. Fig. 6 displays a burial history diagram at Apeldorn Z2 showing thermal maturity evolution. The first noticeable maturity increase is to be found in the Middle Triassic succession, i.e., in the Middle Buntsandstein reservoir. Here, the coalification increasing from 1.1% Rr at the bottom of the top reservoir horizon prior to the heat flow event to 1.2% Rr postdating the event. A similar case scenario can be observed at the top and bottom of the Muschelkalk succession with a clear maturity

https://doi.org/10.1017/S0016774600022873 Published online by Cambridge University Press

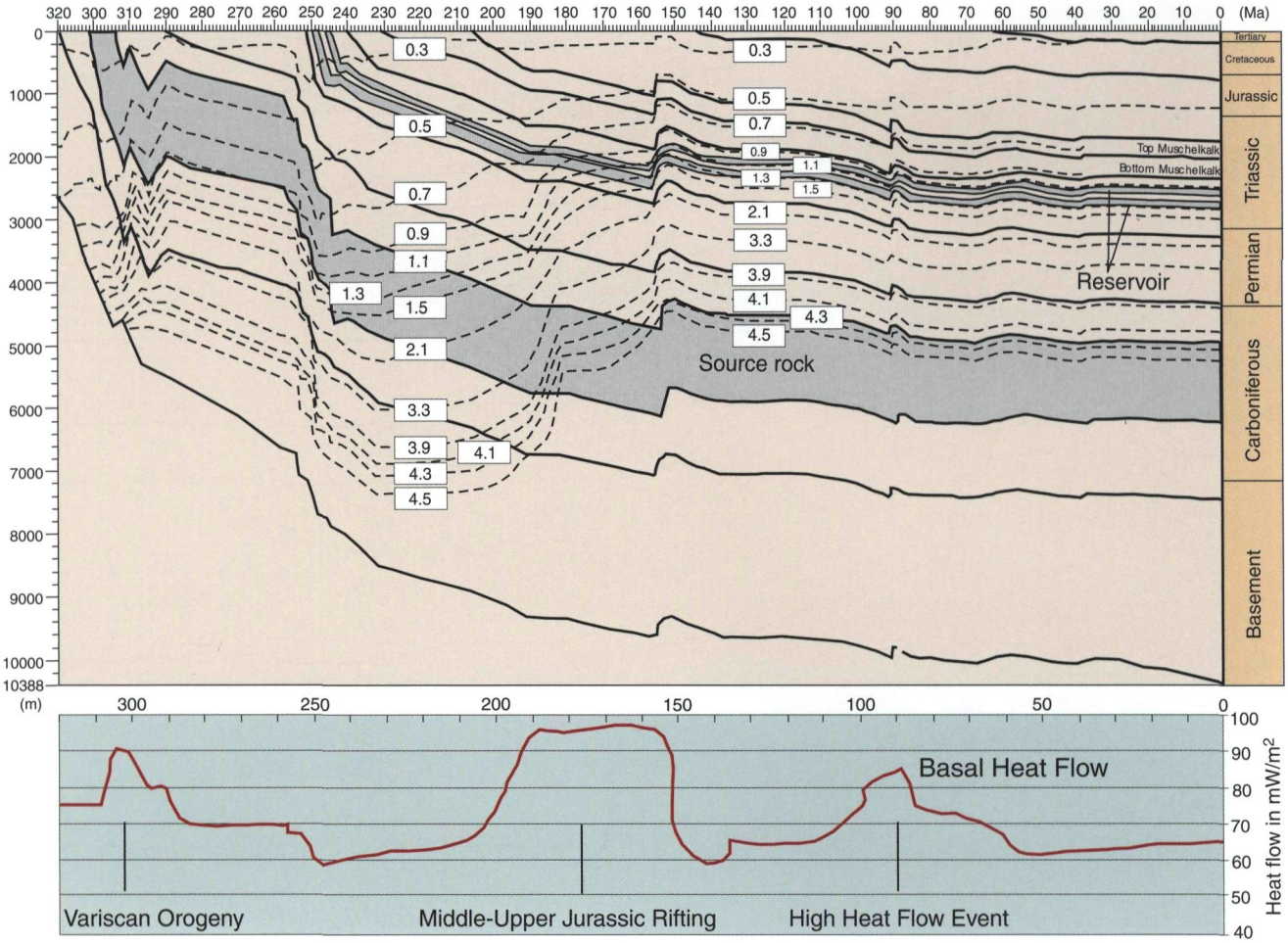

Fig. 6. Burial history diagram, vertical maturity distribution and heat flow history (High heat flow model, scenario 4) at Apeldorn Z2 well.

increase at the bottom succession from 0.9% Rr prior to high heat flow event to 1.0% Rr postdating it and for the top succession from 0.7% Rr prior to it to 0.8% Rr postdating it. The corresponding temperature change in the Middle Buntsandstein reservoir ranged from 80 - 90° C in Albian prior to the Coniacian high heat flow event to 120 - 140° C during the high heat flow event.

In the Lower Jurassic sedimentary units a change in maturation manifests itself in the increase of calculated vitrinite reflectance from 0.55% Rr prior to Coniacian to 0.65% Rr subsequently to it. The corresponding temperature change in the Lower Jurassic sediments ranged from 60° C at Cenomanian prior to the Coniacian high heat flow to ca. 70° C during the Coniacian-Danian period (Fig. 5).

Fig. 7 shows present day modelled and calibrated maturity distribution (Rr %) along the cross-section AA'. The present day maturity distribution is calibrated along the entire section in accordance to the heat flow and burial model displayed in the Table 4. The 2D calibration was performed utilising the following calibration wells: Apeldorn Z2, Lahner Heide 1, Lahn Z1 and Börger 12. Along the cross-section AA', a distinctive lateral maturity trend can be recognised in the entire overburden. This trend is expressed by the distinctive position of the iso-reflectance lines. It shows a moderate to high increase of the present day maturity at top Carboniferous level towards the south-west of the cross-section. In the south-western part of the section, the modelled vitrinite reflectance value amounts to 3.5% Rr at 5100 m, whereas in the deepest part of the section, at 6250 m, it increases up to 4.5% Rr. Further towards northeast, the maturity decreases to 3.18% Rr at 4132 m at Apeldorn, and increases slightly to 3.48% Rr at Lahn Z1 at a depth of 4352 m. The much lower vitrinite reflectances of 2.12 and 2.53% Rr obtained at Apeldorn Z2 well at a depth of 4115 and 4111 m respectively, were measured at vitrinite macerals of poor quality and are therefore not suitable for the above comparison. Even further towards north-east, the coalification of top Carboniferous decreases rapidly through 2.1% Rr at 45,000 m distance and depth of ca. 4000 m to increase at the north-eastern edge to 2.5% Rr and depth of ca. 4100 m. Apart form the modelled present day lateral maturity trend recorded along the entire section, an unusual anticlinal maturity structure can be observed at Apeldorn. Here, a clear 'up-doming' of the iso-reflectance lines depicts an increase of vitrinite reflectance at a depth from ca. 2400 m to ca. 6000 m and is a direct consequence of the thermal perturbances attributed to the salt diapir. In addition, the maturity vs. depth profiles at

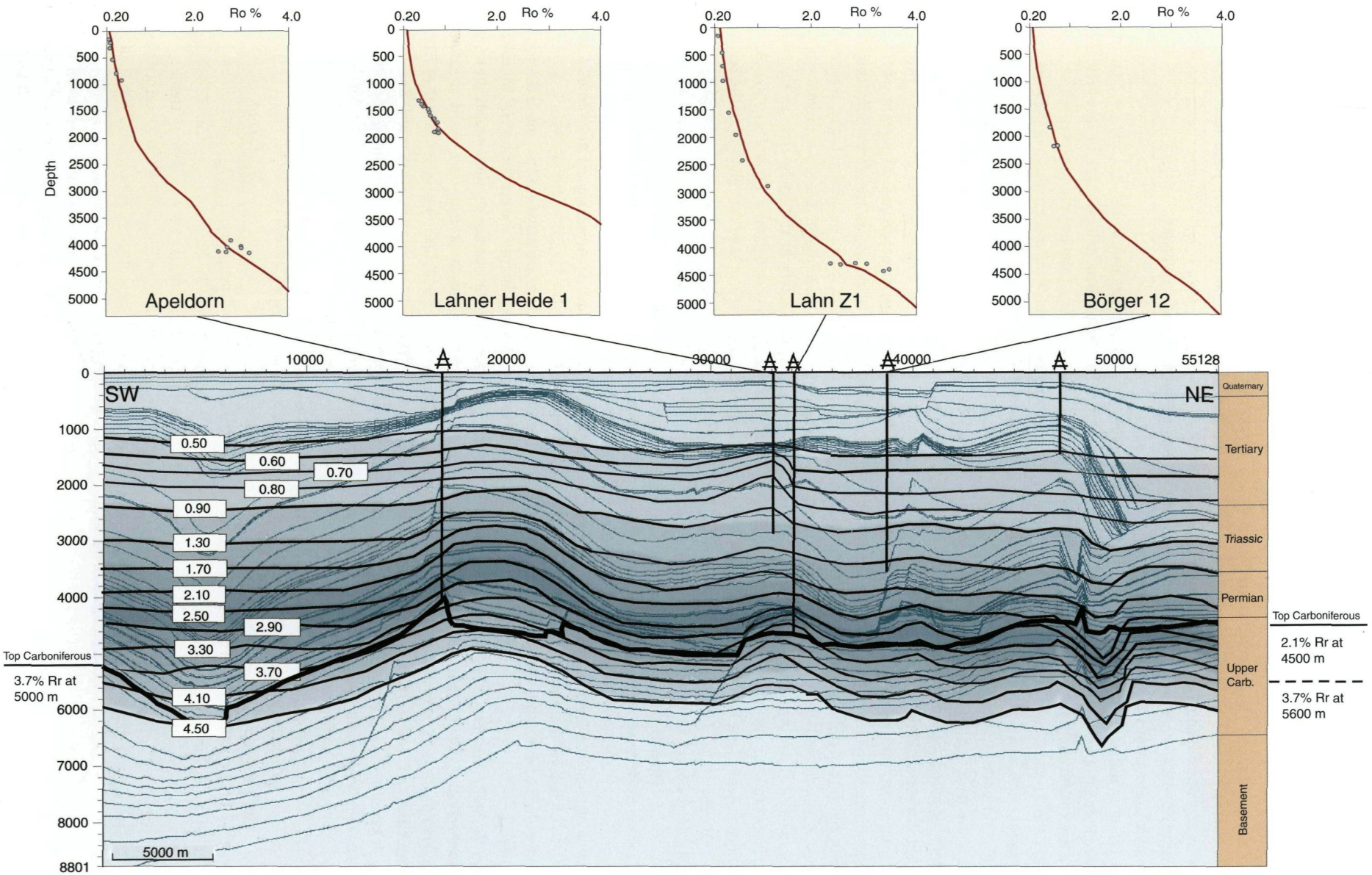

Fig. 7. 2D present day maturity profile AA' with iso-reflectance lines. The maturity pattern at top Carboniferous indicates an overall SW increase in the maturity from 2.1% Rr at 4500 m in the northeast to 3.7% Rr at 5000 m in the south west. At the Apeldorn anticlinal structure, an increase in vitrinite reflectance is clearly visible. 1D maturity curves at Apeldorn, Lahner Heide 1, Lahn Z1 and Börger 12 were utilised in the 2D calibration of the thermal maturity.

both, the Lahner Heide 1 and Lahn Z1 wells, a clear discrepancy in the trend of the maturity curves can be observed. Although, Lahn Z1 well is the only well positioned 2.6 km south east of the studied cross-section AA', its location on the same structural high as Lahner Heide 1, namely the Sögel-Wachtum-Benstrup High, may not necessary invoke the same similarities in the maturity trend as at Lahner Heide 1 well. On the other hand, the distinct maturity differences may be site specific and relate to pre-requisite conditions at both well locations.

The calculation of coalification gradients at a depth range of 1000 to 2500 m for the above wells along the cross-section AA' results in a low coalification gradient of 0.026% Rr/100 m at Apeldorn Z2, Lahn Z1 and Börger 12 and in an even higher coalification gradient of 0.04% Rr/100 m at Lahner Heide 1.

Given the inherent uncertainties of the corrected BHT data derived for the above wells and the Vrees 1 well (Fig 3), only a general statement regarding the temperature profile well can be made. The present day corrected temperature values at Apeldorn are positioned underneath the averaged temperatures collected for Emsland region indicating an overall higher increase in the temperature with depth then for the averaged temperatures in Emsland region. Apeldorn well location on a characteristic structural high and in a closer vicinity of a deep seated fault structure contributes towards the higher temperature profile.

The present day modelled heat flow values reveal an increase of the recent heat flow from 50 mW/m^2 at Lahner Heide 1, through 55 mW/m^2 at Börger 12 to a value of 65 mW/m^2 at Apeldorn and Lahn Z1 (Table 4).

Only at the Lahner Heide 1 well, present day heat flow shows an inverse correlation with the overall coalification gradient. Its heat flow value of 50 mW/m^2 may be explained in terms of the cooling effect of descending waters, migrating downdip along faults, fractures and fissures decreasing the overall temperature field.

At Apeldorn Z2 well, the maximum burial depth of ca. 7000 m was reached twice, for the first time shortly prior to the Middle-Upper Jurassic rifting event and for the second time shortly prior to the Coniacian-Santonian inversion. The corresponding maximum burial temperatures prior to the Middle-Upper Jurassic rifting event were attained in Oxfordian, ca. 155 Ma ago and amounted to ca. 360° C whereas burial temperatures prior to the Coniacian-Santonian inversion amounted to 340° C.

Effects of the Upper Cretaceous Inversion on the gas prone system of the gas field Apeldorn

Gas generation and migration

Based on the 2D basin modelling results, first methane expulsion from the Westphalian A took place in late Westphalian times, i.e. 302 Ma ago. At the beginning of Keuper, ca. 231 Ma (Fig. 8), a renewed generation and expulsion of methane sourced from Westphalian source rocks took place along the entire cross-section AA'. This marked a second phase of methane generation from the gas prone Westphalian source rocks.

At the same time, 231 Ma ago methane entered and began to saturate for the first time available pore space within the Zechstein and Rotliegend successions. At present, there is no indication of trap existing within the successions of Permian age. However, given a great number of gas reservoirs at Zechstein and fewer at Rotliegend level, a presence of such entrapments is more likely in the study area, to the west of the Ems River. In the late Liassic (Toarcian), 180 Ma ago, further re-migration of methane took place into the Zechstein overburden. The hydrocarbon generation potential of Westphalian source rocks became exhausted 154 Ma ago.

Nitrogen expulsion from Westphalian A, B and C started 200 Ma ago, in the late Triassic (Fig. 8). In the Late Liassic (180 Ma) 6 to 13% of the pore space of Permian successions were saturated with nitrogen, increasing to 20 to 35% in the Late Jurassic.

During the Upper Cretaceous inversion, an extensive free gas exsolution from formation waters within the Westphalian source rock units and the overburden were modelled caused by reduction of the hydrostatic pressure as a result of structural uplift (Cramer et al., 2002). Fig. 9 displays modelled free gas exsolution effect in the entire overburden due to the structural uplift at the Apeldorn well during the Coniacian-Santonian inversion at 87 Ma.

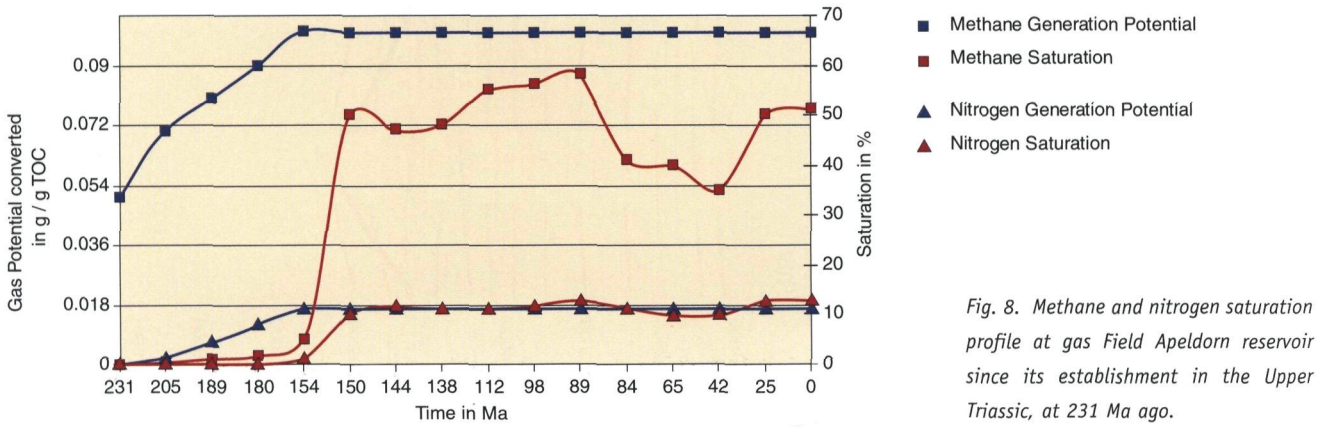

Fig. 8. Methane and nitrogen saturation profile at gas Field Apeldorn reservoir since its establishment in the Upper Triassic, at 231 Ma ago.

Reservoir saturation

According to the modelling results, pore space within the gas Field Apeldorn began to be saturated by methane for the first time 154 Ma ago in the Oxfordian as a result of secondary migration of methane, (Fig. 8). The gaseous hydrocarbons of Westphalian origin were sourced from already established hydrocarbon pools present at Upper Rotliegend level as opposed to be sourced directly from the Westphalian source rock. The above saturation at Apeldorn gas reservoir with methane sourced directly from the methane pools at Rotliegend level relates to the exhausted methane generation potential of the Westphalian source rocks in early Malm (Oxfordian), 154 Ma ago. Therefore, methane generation within the Westphalian source rock units became depleted at the same time as methane began to saturate the gas field Apeldorn for the first time i.e., at 154 Ma. Major methane dismigration from Upper Rotliegend into the Triassic reservoir took place along fault zones during the phase of fault opening set in Late Triassic – Jurassic (205 - 112 Ma). Only a minor amount of methane entered the reservoir via vertical migration through the sedimentary overburden.

First nitrogen entrapment in the gas field Apeldorn took place in the Lower Cretaceous, 130 Ma ago.

The modelled structural integrity of the fault seal at gas field Apeldorn was severely affected by reactivation of basement faults due to the Coniacian-Santonian inversion. Seal failure due to intensive fault reactivation resulted in remigration of methane and nitrogen during the Late Cretaceous. The associated decline in the modelled methane saturation within the Triassic reservoir, which proceeded until the late Coniacian times, was a direct consequence of the applied fault seal model.

At the start of the Upper Cretaceous inversion phase, methane saturation amounted to ca. 59 % at 89 Ma (Fig. 9). During the inversion episode, methane saturation decreased to ca. 43% at 84 Ma as seen in Fig. 8. Due to the Coniacian-Santonian inversion, the remaining methane mixed with the hydrostatic free gas released from formation waters at the Apeldorn gas reservoir. Prior to the Upper Cretaceous inversion the pore space saturation with nitrogen gas reached a maximum of 12% decreasing to 0.5 - 1.5% at 87 Ma during the Coniacian-Santonian inversion event.

At 42 Ma modelled methane saturation increased to 35% whereas at present the modelled saturation reaches a value of 51% of the pore space. At present, nitrogen saturation amounts to ca. 12 - 13%.

Prior to the Upper Cretaceous inversion, the burial depth to which the gas prone Westphalian source rocks became subjected amounted to ca. 5000 m. Due to the above inversion, the same source rocks experienced a tectonic uplift on average of ca. 500 m and to a maximum of 800 m along line AA'.

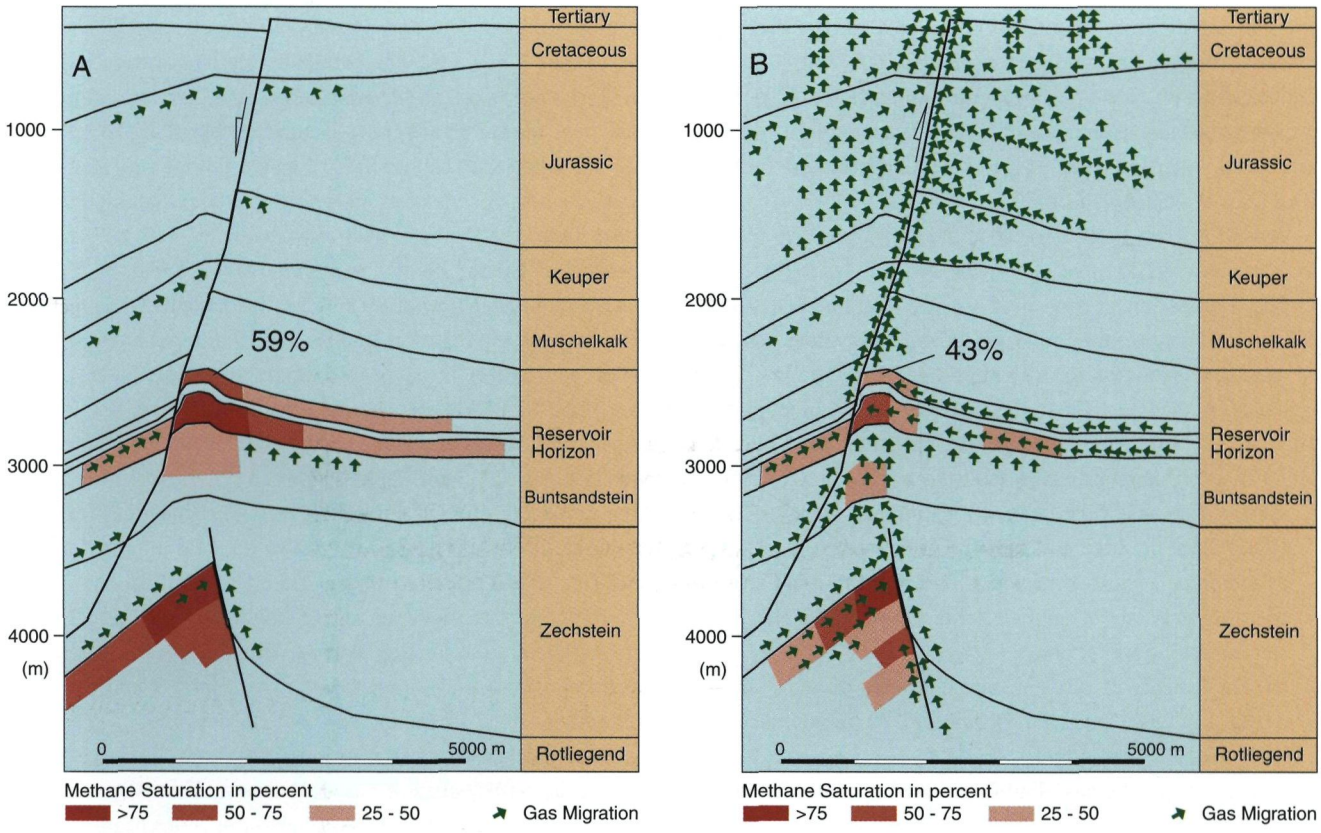

Fig. 9. Migration of methane and saturation of the pore space with methane (in percent of total volume) at gas field Apeldorn (two reservoir horizons in the Buntsandstein) preceding (A) and during the Coniacian-Santonian inversion (B). Detailed geological sections are based on the cross-section AA' (Fig. 2).

https://doi.org/10.1017/S0016774600022873 Published online by Cambridge University Press

Discussion

Thermal impact, which can originate from any kind of thermal source, can be reconstructed by determination the palaeoheat flow history in the study area. Palaeoheat flow history can be constrained by means of various maturity indicators, such as vitrinite reflectance, fluid inclusion or for e.g., apatite/zircon fission track data.

Utilising various maturity indicators in a procedure of thermal calibration, one can point towards minor and major alterations to the palaeoheat flow history. Schmidt-Mumm (1995) conducted a number of fluid inclusions analyses at well Apeldorn Z2. According to his results, samples of Upper Carboniferous to Middle Triassic age were marked by formation of distinct fluid inclusions, which can be indirectly related to two diagenetically different mineral phases occurring in sedimentary and volcanic successions. Although lacking the direct control on the timing of the fluid inclusion formation, Schmidt-Mumm (1995) implied that two major diagenetic phases were discerned reflecting the regional subsidence of the LSB and the Subhercynian basin inversion. These diagenetic phases mark the homogenisation temperature at base Permian of 165° C for the period of regional subsidence and of 180 - 210° C for the period of Cretaceous basin inversion. The temperature range of 180 - 210° C discriminated for the period of Subhercynian basin inversion compares very well with the modelled temperature of 200° C at well Apeldorn whereas temperature of 165° C determined for the basin subsidence correlates broadly with modelled 140 - 200° C, seen in Fig. 5. In result, elevated temperatures of 180-210° C determined by the above analysis of fluid inclusions for a period of structural inversion support the modelled elevated temperature field at well Apeldorn Z2.

Apatite/zircon fission track data were not at the disposal for the above study area.

The application of measured vitrinite reflectance data in calibration study resulted in elevated heat flow values according to the best scenario of the high heat flow-shallow burial model at Apeldorn, Lahner Heide 1, Lahn Z1 and Börger 12. The best-fit scenario between the measured and modelled vitrinite reflectance values is achieved by:

- setting the heat flow value to 95 mW/m^2 during Middle-Upper Jurassic Rifting at all respective wells;
- by assigning a short-termed heat flow event during Coniacian with 120 mW/m^2 at Lahner Heide 1 and to 85 mW/m^2 at the remaining wells; and
- by application of shallow burial model of max. 400 m during the basin inversion phase, i.e., during Coniacian.

Application of the modelled Coniacian high heat flow event at the Apeldorn Z2 well resulted in alteration of the thermal regime and maturity distribution. For e.g., temperature at Middle Buntsandstein reservoir changed from 80 - 90° C in Albian, prior to the Coniacian high heat flow event to 120 - 140° C in Coniacian during the high heat flow event. A similar scenario applies to the top Carboniferous with a temperature increase from 160° C in Albian to 200° C in Coniacian. With regard to the thermal maturity at Apeldorn Z2 well, neither application of the Coniacian high heat flow event nor the Upper Cretaceous-Tertiary burial did have a quantifiable effect on maturity distribution within the Carboniferous and Permian successions. As a result, coalification level within the Carboniferous and Permian successions remained unaltered during the applied Coniacian high heat flow event. This is in addition also confirmed by both, the high vitrinite reflectance values of 3.18 - 4.5% Rr at the top Carboniferous together with the low coalification gradient of 0.029 - 0.04% Rr/100 m (1000 - 2500 m), which exclusively points towards a burial model without the necessity of Coniacian high heat flow event.

On the contrary, application of the Coniacian high heat flow event does have however a clear impact on the thermal maturity of the top Middle Buntsandstein reservoir as well as younger Mesozoic and Cenozoic successions. The corresponding changes within the Middle Buntsandstein reservoir to thermal maturity amount to 1.1% Rr prior to the Coniacian heat flow event and to 1.2% Rr postdating the high heat flow event. Similar changes apply to younger successions.

Present day corrected BHT measurements show the highest temperature deviations for Apeldorn indicating an overall higher increase in the temperature with depth than for the averaged temperatures in Emsland region. The present day BHT records at Lahner Heide 1 do not permit a coherent statement. With respect to the present day heat flow regime, the highest present day heat flow of 65 mW/m^2 was modelled again at the Apeldorn Z2 well whereas at Lahner Heide 1 a heat flow of only 50 mW/m^2 was attained. With regards however to the Coniacian high palaeoheat flow, the highest heat flow value of 120 mW/m^2 was derived at Lahner Heide 1 well, whereas at Apeldorn Z2, only an elevated heat flow of 85 mW/m^2 was modelled. In addition, the highest coalification gradient for the depth interval from 1000 to 2500 m is calculated again at Lahner Heide 1 and amounts to 0.04% Rr/100 m. The coalification gradient at Apeldorn Z2 well amounts to only 0.029% Rr/100 m. The inverse relationship at Lahner Heide 1 between the highest heat during the Coniacian and the lowest present day modelled heat flow value might be explained in terms of the cooling effect attributed to the descending waters circulating within the highly faulted and fractured deep seated inverted graben structure at Lahner Heide. Descending waters, which are derived from the surface and flush the underlying formations are know to have a cooling effect on the overall heat flow regime.

Further, the inverse relationship at Apeldorn Z2 well between the highest BHT, present day heat flow and the slightly lower Coniacian heat flow might be explained in terms of its location on a structural high, close to a deep rooted fault and being overlain by a salt diapir.

The thermal calibration method utilising various thermal maturity indicators does not differentiate between the specific heat flow source with regard to the applied changes in the palaeo-heat flow history.

The possible source of the applied elevated (85 mW/m^2) and high (120 mW/m^2) basal heat flow during Coniacian might be related to the intra-plate phenomenon of basin inveresion. After the theory of P.A. Ziegler (Ziegler, 1987a,b; Ziegler et al., 1995), basin inversion in Northern Europe resulted from the compressional phase and crustal shortening caused by the continent-continent collision of the African with the Euroasian plate with its front is located at the northern margin of the Alps and the Carpathians. The respective stress transfer mirrored by the development of collisional intra-plate deformation structures can occur after Ziegeler (1998) at distances of up to 1600 km from a collision front and with it of course the intrinsic change in the rheology at the mantle-lithosphere level. Hansen & Nielsen (2001) support these changes by modelling the processes of basin inversion. The reactivation of sedimentary basins in compression generated shorthening, thickening of the crust and uplift followed by erosion. In response to loading of the thickend sediments and crust, the upper mantle subsides in the central part of the basin.

Even further, Pratt (2000) points out that mantle heat flow and material transport can cause significant changes in crustal thickness, composition, and density. This is also emphasized by a number of alternative models to plate tectonics such as the model of endogenous regimes (Pavlenkova, 1995, 1998). It is therefore plausible to assume that a major change in the mantle heat flow at a depth for e.g., of 140 km (Neugebauer & Reuther, 1987) could have led to a distinct change of the geothermal regime within the lower and upper crust of the LSB without necessary invoking a shallow intrusive body (5 - 6 km, Brockamp, 1967).

A number of basin modelling simulation studies have also attemted to explain the anomalous thermal maturity pattern observed in the LSB (Fig. 5). Stadler & Teichmüller (1971), Buntebarth & Teichmüller (1979) and Buntebarth (1985) calculated a heat flow of 150 mW/m^2 for a time span of 7.7 Ma during Turonian-Coniacian time in accordance to an empirically derived function. Further, Düppenbecker (1991) modelled a heat flow of 65 - 82 mW/m^2 and 71.4 - 131 mW/m^2 at two wells in the Emsland region for the time span of 78 - 97 Ma during Late Turonian. In addition, Leischner (1994) calculated heat flow values of 84 mW/m^2 for the time span of 91 - 85 Ma during Late Turonian-Santonian, and with a peak at 88 Ma. Finally, Petmecky et al. (1999) explained the thermal maturity pattern in the centre of the LSB solely by the application of the deep burial in the centre of the LSB.

Apart from the gravity and magnetics anomalies occurring in the LSB, (Reich, 1933; Hahn et al., 1971; Plaumann, 1983, 1991; Bachmann & Grosse, 1989; Hermes, 1986; Giebler-Degro, 1986; Giebler-Degro et al., 1986) and refraction seismics (Nodop, 1971 and Thyssen et al., 1971), presence of Upper Cretaceous, intrusive bodies (see Fig. 1), is inferred based on a number of the following indicators:

- Carboniferous coals have reached the meta-anthracite degree of coalification in the Westphalian D of the Piesberg area (4.8% Rr, 6.8% R_{max} at surface), (Teichmüller et al., 1984).
- Dehydratisation of Cretaceous coals at depths of 2000 - 3000 m above the postulated Bramscher Massif. Following Stadler & Teichmüller (1971), 300° C are necessary for this alteration, which would require a subsidence in the order of 10,000 - 12,000 m at a normal thermal gradient (2 - 3° C/ 100 m).
- Moreover, temperature sensitive authigenic albite in the Muschelkalk overlying the postulated Vlotho massif required high formation temperatures of ca. 300° C (Fabian 1971).
- Saxonian Ba, Pb & Fe mineralization and other mineralogical indicators such as pyrophyllite were reported by Tischendorf (1987), Büchner & Seraphim (1977), Stadler & Teichmüller (1971), Patniak & Füchtbauer (1975), Schreyer (1968) and Schreyer (1969).
- Iron ore formation in the Buntsandstein fault and fracture zones (Büchner & Seraphim, 1977) are documented in the high coalification area of Piesberg and the postulated Vlotho Massif.
- High illite-, chlorite- and pyrophyllite- crystalinity in the biocalcarenites of the Upper Muschelkalk (Teichmüller et al., 1979 and Deutloff et al., 1980; Brauckmann, 1984; Richter et al., 1986). Temperature regime of 220 - 330° C for growth of high temperature illite and ca. 200° C for chlorite is necessary.
- Contact metamorphism in Valendis deposits of the Sulingen oil field on the northern rim of the LSB (Stadler & Teichmüller, 1982).
- Chlorite crystalinity in the Mesozoic Schwarzschiefer (Black Shales), overlying the postulated Vlotho massif indicates thermal diagenesis to anchi-metamorphism, (Fabian, 1971).
- Positive gravity and magnetic anomalies led to the postulation of the associated intrusive body of Bramsche (Reich, 1933) and the other Cretaceous intrusions (Bachmann & Grosse, 1989; Hermes, 1986; Giebler-Degro, 1986; Giebler-Degro et al., 1986; Plaumann 1983, 1991).
- Anomalous coalification values were encountered by numerous authors: Teichmüller & Teichmüller (1950, 1951), Stadler & Teichmüller (1971), Buntebarth & Teichmüller (1979), Bartenstein et al. (1971), Koch & Arnemann (1975), Deutloff et al. (1980).

Apart from the modelled thermal effects of the inferred intrusive bodies, the Upper Cretaceous inversion had a considerable influence on the Mesozoic petroleum system, i.e. on the respective gas composition and distribution at gas field Apeldorn. The structural uplift resulted in trap destruction at

https://doi.org/10.1017/S0016774600022873 Published online by Cambridge University Press

gas Field Apeldorn. It led to a severe seal breaching, induced by reactivation of fault structures during the Upper Cretaceous inversion. As a result, methane saturation in the Lower Buntsandstein reservoir of the gas field Apeldorn decreased from 55% at Turonian (89 Ma) prior to the inversion to ca. 28% in Santonian (87 Ma) post the inversion. Similarly, nitrogen saturation displayed a major decline from 12% at 89 Ma to 0.5 - 1.5% at 87 Ma. Apart from the trap destruction, another major effect of the Coniacian-Santonian inversion is indicated by the hydrostatic exsolution. The liberation of free gas exsolving from formation waters of the neighbouring successions took place as a direct consequence of change to temperature and pressure conditions due to the structural inversion and uplift.

The present anomalous nitrogen content of 75% (Vol.) and methane content of and 24% (Vol.) could not be satisfactory reproduced during the consequent simulation runs. Two scenarios could explain the achieved results:

- Suitability of the applied simple fault model.
- Three dimensionality of geochemical processes as intricate settings influenced by both, structural inversion and high heat flow events may inhibit simulation performance of geochemical processes.

The next aspect is whether and how the reservoir content agrees with the geological evolution of the gas field and in particular with the structural inversion:

- Stable carbon isotope ratios of methane are heavy (>–20‰) *therefore clearly indicating a gas trapping mechanism* exclusively from a highly mature coal. This, on the other hand, excludes the existence of any significant part of gas generated earlier.
- There is a large discrepancy between the modelled nitrogen saturations and nitrogen contents in the Apeldorn gas field as observed today. In consequence, the high nitrogen content in the field cannot be explained by the model of biogenic nitrogen production applied here. The additional amount of nitrogen not covered by the model might originate from an admixture from abiogenic sources, probably related to the tectonic history of the setting. This might be supported by the fact, that nitrogen contents in natural gas reservoirs surrounding the massifs increase with their decreasing distance from the intrusives. Gerling et al. (1997, 1999) estimated that the nitrogen most probably derives from an inorganic source, either from the deeper crust or even from the upper mantle.
- A regional 'CO_2-anomaly' in natural gases provides independently of reservoir age yet another indication for the existence of the Bramsche Massif (e.g. Brand et al., 1983; Gerling et al., 1995, 1999 and Lokhorst et al., 1998): CO_2 correlates with the maturity map – Upper Cretaceous intrusives are clearly marked by high CO_2 contents, locally above 10%.
- The latter suggestion is additionally supported by the fact that up to 3% primordial He was detected in several natural gas reservoirs northwest of the Uchte massif (Gerling et al., 1994).
- The only gas data, which do not clearly confirm the existence of the Upper Cretaceous intrusive body, are stable carbon isotope ratios of ethane and propane. Those data indicate a source rock maturity below 2% vitrinite reflectance. However, one has to consider that those gases occur only in minor quantities (<500 ppm) and that these amounts could either be a remaining part of a pre-inversion reservoir fill or could be derived from free gas exsolving from surrounding formation waters.

Conclusion

A 2D forward basin modelling study of the Palaeozoic system was performed at gas field Apeldorn in the Emsland region. It assessed thermal influence of the modelled Coniacian high heat flow event on the maturity distribution and the effect of the Upper Cretaceous inversion on the HC generation, migration and fill of the Lower Triassic Buntsandstein reservoir located at the western rim of the inverted Lower Saxony Basin.

Application of the Coniacian basal high heat flow event together with a shallow burial scenario of max. 400 m according to the palaeogeographic reconstructions satisfies the fit between the measured and modelled vitrinite reflectance. It supports the hypothesis of a high heat flow event giving rise to quantifiable thermal alterations in Mesozoic successions (Lower Triassic and younger) postulated on the account of the Apeldorn intrusive off-shoot body. It however does not conform to the high vitrinite reflectance at top Carboniferous as caused by the applied Coniacian high heat flow event. Results of the thermal calibration point namely towards an elevated maturity at the top Carboniferous being attained immediately prior to the Middle-Upper Jurassic rifting event and as a result of Permian-Triassic burial. Thermal maturity at top Carboniferous succession is therefore lacking any assessable thermal 'imprint' that could have been attributed to the applied Coniacian high heat flow event.

With regards to the effects of the Upper Cretaceous inversion on the charge history of the gas field Apeldorn, the simulated model conforms to the already established conventional qualitative statements. The coal-derived Westphalian source rocks of the Palaeozoic Petroleum System experienced two phases of methane generation: in late Westphalian and in Keuper times, respectively.

The Triassic Buntsandstein gas reservoir of the Apeldorn field became saturated with methane for the first time in Oxfordian and with nitrogen in Lower Cretaceous. During the Coniacian-Santonian inversion, a very extensive free gas exsolution was modelled within the Westphalian source rock and

the adjacent strata as well as within the Triassic gas reservoir. The decrease in methane and nitrogen saturation at the gas field Apeldorn was a direct consequence of the structural uplift and inversion. Moreover, free gas exsolving from formation waters of the reservoir and the adjoining Palaeozoic strata mixed with the remaining methane and nitrogen accumulation at the Apeldorn gas field.

Acknowledgements

The authors would like to thank Gaz de France Deutschland GmbH, Germany (formerly Preussag Energie GmbH, Germany), BEB Erdgas und Erdöl GmbH, Germany, Mobil Erdgas-Erdöl GmbH, Germany & RWE Dea AG for providing significant geological and geochemical information and for their permission to publish. Valuable discussion during the study carried out as well as assistance by Dr. C. Büker is greatly appreciated. The authors are thankful to Dr. P. Gerling for valuable contributions on isotope and gas geochemistry. Dr. H. J. Koch (BGR) provided essential organic petrography guidance and supplied vitrinite reflectance data. The authors are much indebted to the constructive suggestions made upon the first version of the manuscript by Dr. W. Viesser and Dr. Simmelink.

References

Bachmann, G.H. & Grosse, S., 1989. Struktur und Entstehung des Norddeutschen Beckens – geologische und geophysikalische Interpretation einer verbesserten Bouguer – Schwerkarte. *In:* Das Norddeutsche Becken – Geophysikalische und geologische Untersuchungen des tieferen Untergrundes. Niedersächsische Akademie der Geowissenschaften. Veröffentlichung 2: 23-47.

Baldschuhn, R., 1996. Geotektonischer Atlas von Nordwest-Deutschland, Blatt Nordhorn C 3506, Das Schollenmuster im Sockel NW-Deutschlands: 1: 1 000 000. BGR, (unpublished report), Nr.: 00704561.

Baldschuhn, R. & Kockel, F., 1994. Geotektonischer Atlas von NW-Deutschland 1: 300 000, 1. abgedeckte geologische Karte der Unterkreidebasis. BGR, (unpublished report) Nr.: 9008905.

Baldschuhn, R. & Kockel, F., 1999. Das Osning-Lineament am Südrand des Niedersachsenbeckens. Zeitschrift der Deutschen Geologischen Gesellschaft 150 (4): 673-695.

Baldschuhn, R., Frisch, U. & Kockel, F., 1985. Inversionsstrukturen in NW-Deutschland und ihre Genese. Zeitschrift der Deutschen Geologischen Gesellschaft 136: 129-139.

Baldschuhn, R., Best, G. & Kockel, F., 1991. Inversion tectonics in the northwest German Basin. *In:* Spencer, A.M. (ed): Generation, Accumulation and Production of Europe's Hydrocarbons. Special Publication of the European Association of Petroleum Geoscientists 1: 149-159.

Baldschuhn, R., Frisch, U. & Kockel, F., 1998. Der Salzkeil, ein strukturelles Requisit der saxonischen Tektonik. Zeitschrift der Deutschen Geologischen Gesellschaft 149 (1): 59-59.

Baldschuhn, R., Binot, F., Fleig, S., Kockel, F., Best, G., Brückner-Röhling, S., Deneke, E., Frisch, U. & Hoffmann, N., 2001. Geotektonischer Atlas von Nordwest-Deutschland und dem deutschen Nordsee-Sektor (Medienkombination), Strukturen, Strukturentwicklung, Paläogeographie. Geologisches Jahrbuch Reihe A 153: 3-95.

Bartenstein, H., Teichmüller, M. & Teichmüller, R., 1971. Die Umwandlung der organischen Substanz im Dach des Bramscher Massivs. Fortschritte in der Geologie von Rheinland und Westfalen 18: 501-538.

Betz, D., Führer, F., Greiner, G. & Plein, E., 1987. Evolution of the Lower Saxony Basin. *In:* Ziegler, P.A. (ed): Compressional Intraplate Deformations in the Alpine Foreland. Tectonophysics 137: 249-256.

Binot, F., Gerling, P., Hiltmann, W., Kockel, F. & Wehner, H., 1993. The Petroleum System in the lower Saxony Basin. *In:* Spencer (ed): Generation, accumulation and production of Europe's hydrocarbons. Special Publication of the European Association of Petroleum Geoscientists 3: 121-139.

Boigk, H., 1952. Aufschlussarbeiten an der Struktur Apeldorn 1944-1952. Niedersächsisches Landesamt für Bodenforschung, (unpublished report), Nr.: 0094550.

Boigk, H., 1981. Erdöl und Erdgas in der Bundesrepublik Deutschland. Felder, Förderung, Vorräte, Lagerstättentechnik. Enke Verlag (Stuttgart): 330 pp.

Brand, E., Fricke, K. & Hedemann, H.A., 1983. Die Vorkommen natürlicher Kohlensäure (CO2) in der Bundesrepublik Deutschland. DGMK-Bericht: Über die Verfügbarkeit von Kohlendioxid zur Ausbeute-Steigerung in Erdöllagerstätten der Bundesrepublik Deutschland 202 (1): 1–118.

Brauckmann, F.J., 1984. Hochdiagenese im Muschelkalk der Massive von Bramsche und Vlotho. Bochumer Geologische und Geotechnische Arbeiten 14: 1-195.

Brink, H. J., 2001. Die Anomalie von Bramsche, wieder eine offene Frage? DGMK – Tagungsbericht 2001 – 2:153-164.

Brockamp, B., 1967. Kurzbericht über die im Gebiet um Osnabrück durchgeführten seismischen Arbeiten des Instituts für Reine und Angewandte Geophysik der Universität Münster. Veröffentlichungen der Deutschen Geodätischen Kommission, 153(B): 1-12.

Brückner-Röhling, Hoffmann, N., Koch, J., Kockel, F., Krull, P & Stumm, M., 1994. Tiefengas, die Struktur-, Mächtigkeits- und Inkohlungskarten des Norddeutschen Oberkarbon- und Permbeckens und seiner Ränder. (unpublished report), Nr.: 00598095.

Büchner, M. & Seraphim, E.T., 1977. Mineralneubildungen im Saxonischen Bruchfaltengebirge des unteren Weserberglandes. Teil 3: Nachträge zu den Lagerstätten und Kausalfrage. Bericht des Naturwissenschaftlichen Vereins für Bielefeld und Umgebung 23: 9-89.

Buntebarth, G. & Teichmüller, R., 1979. Zur Ermittlung der Paläotemperaturen im Dach des Bramscher Intrusives aufgrund von Inkohlungsdaten. Fortschritte in der Geologie von Rheinland und Westfalen 27: 171-182.

Buntebarth, G., 1985. Das Temperaturgefälle im Dach des Bramscher Massivs aufgrund von Inkohlungsuntersuchungen im Karbon von Ibbenbüren. Fortschritte in der Geologie von Rheinland und Westfalen 33: 255-264.

Burnham, A.K. & Sweeney, J.J., 1989. A chemical kinetic model of vitrinite maturation and reflectance. Geochimica et Cosmochimica Acta 53: 2649-2657.

Büker, C., Littke, R. & Welte, D.H., 1996. 2D-modelling of the thermal evolution of Carboniferous and Devonian sedimentary rocks of the eastern Ruhr basin and northern Rhenish Massif, Germany. Zeitschrift der Deutschen Geologischen Gesellschaft 146 (2): 321-339.

Cramer, B., Schlömer, S. & Poelchau, H. S., 2002. Uplift-related hydrocarbon accumulations: the release of natural gas from groundwater. *In:* A.G. Dore, J.A. Cartwright, M.S. Stoker, J.P. Turner, N. White (eds): Exhumation of the North Atlantic margin: timing, mechanism and implications for petroleum exploration. Geological Society, London, Special Publications 196: 447-455.

Deutloff, O., Teichmüller, M., Teichmüller, R. & Wolf, H., 1980. Inkohlungsuntersuchung im Mesozoikum des Massivs von Vlotho (Niedersächsisches Tektogen). Neues Jahrbuch für Geologie und Palaeontologie 1980: 321-341.

Drozdzewski, G., 1992. Zur Faziesentwicklung des Oberkarbon des Ruhrbeckens, abgeleitet an Mächtigkeitskarten und lithostratigraphischen Gesamtprofilen. Zeitschrift für Angewandte Geologie 38 (1): 41-48.

Düppenbecker, S.J., 1991. Genese und Expulsion von Kohlenwasserstoffen in zwei Regionen des Niedersächsischen Beckens unter besonderer Berücksichtigung der Aufheizraten. Berichte des Forschungszentrums Jülich, 2657, 304 pp.

Faber, E., 1987. Zur Isotopengeochemie gasförmiger Kohlenwasserstoffe. Erdöl, Erdgas, Kohle 103(5):210-218.

Fabian, H.J., 1971. Die Aufschlussbohrung Ellerburg Z1 bei Lübbecke in Westfalen. Fortschritte in der Geologie von Rheinland und Westfalen 18: 423-428.

Franke, D., Hoffmann, N. & Lindert, W., 1995. The Variscan deformation front in East Germany, Part I: geological and geophysical constraints. Zeitschrift für Angewandte Geologie 42 (2): 83-91.

Franke, D., Hoffmann, N. & Lindert, W., 1996. The Variscan deformation front in East Germany, Part II: Tectonic interpretation. Zeitschrift für Angewandte Geologie 42 (1): 44-56.

Friberg, L.J., 2001. Untersuchungen zur Temperatur- und Absenkungsgeschichte sowie zur Bildung und Migration von Methan und molekularem Stickstoff im Nordostdeutschen Becken, Berichte des Forschungszentrums Jülich: 391: 1-249.

Gerling, P., Kockel, F. & Krull, P., 1994. Prä-Westfal-Play in Nord-Deutschland – Pilotstudie in Vorbereitung einer Fortsetzung des Verbundforschungsvorhabens 'Tiefengas' – BGR, (unpublished report), Nr.: 112.283.

Gerling, P., Mittag-Brendel, E., Sohns, E., Faber, E. & Wehner, H., 1995. Tiefengas: Genese und Verteilungsmuster der Erdgase im Norddeutschen Becken. – BGR, (unpublished report), Nr.: 112440.

Gerling, P., Idiz, E., Everlien, G. & Sohns, E., 1997. New aspects on the origin of nitrogen in natural gas in Northern Germany. – Geologisches Jahrbuch D103: 65-84.

Gerling, P., Geluk, M.C., Kockel, F., Lokhorst, A., Lott, G.K. & Nicholson, R.A., 1999. NW European Gas atlas – New implications for the Carboniferous gas plays in the western part of the Southern Permian Basin. *In:* Fleet, A.J. & Boldy, S.A.R. (eds): Petroleum Geology of Northwest Europe, Proceedings of the 5th Conference. Geological Society, (London): 799-808.

Giebler-Degro, M., 1986. Zur Tiefenerkundung des Niedersächsichen Tektogens durch dreidimensionale Simulationsrechnungen. TU Clausthal, Unpublished PhD-Thesis: 203 pp.

Giebler-Degro, M. & Götze, H-J., 1986. Dreidimensionale gravimetrische und magnetische Modellrechnngen zur Erfassung des tieferen Untergrundes im südlichen Norddeutschen Becken. T.U. Clausthal (unpublished report): 1-54.

Graßmann, S., Cramer, B. & Winsemann, J., 2003. Erdölgeologische Modellierung der Lagerstätte Bramberge, Emsland. DGMK Tagungsbericht 2003 (1): 109-116.

Gramann, F., Heunisch, C., Klassen, H., Kockel, F., Dulce, G., Harms, F.-J., Katschorek, T., Mönning, E., Schudack, M., Schudack, U., Thies, D., Weiss, M. & Hinze, C., 1997. Das Niedersächsische Oberjurabecken - Ergebnis interdisziplinärer Zusammenarbeit. Zeitschrift der Deutschen Geologischen Gesellschaft 148 (2): 165-236.

Hahn, A. & Kind, E.G., 1971. Eine Interpretation der magnetischen Anomalie von Bramsche. Fortschritte in der Geologie von Rheinland und Westfalen 18: 387-394.

Hansen, D.L. & Nielsen, S.B., 2001. Modelling process of basin inversion. European Union of Geosciences. EUG XI MEETING 8th – 12th April 2001, Strasbourg – France, Symposium LS05-The dynamics of basin inversion: Observation and Numerical Modelling.

Haenel, R., 1980. Atlas of subsurface temperatures in the European Community. Kommission der Europäischen Gemeinschaft, EU 6578: 1-36.

Hermes, H.J., 1986. Calculation of pre-Zechstein Bouguer anomaly in northwest Germany. First Break 4, (11): 13-22.

Hoffmann, N., Fluche, B. & Jödicke, H., 1995. Neuerkenntnisse zur tektonischen Felderung des tieferen Untergrundes im Norddeutschen Becken – ein Ergebnis magnetotellurischer Messungen. Nachrichten der Deutschen Geologischen Gesellschaft 54: 85-86.

Hoffmann, N., Stiewe, N. & Pasternak, G., 1996. Struktur und Genese der Mohorovicic – Diskontinuität (Moho) im Norddeutschen Becken – ein Ergebnis langzeitregistrierter Steilwinkelseismik. Zeitschrift für Angewandte Geologie 42 (2): 138-148.

Hoffmann, N., Jödicke, H., Fluche, B., Jording, A. & Müller, W., 1998. Modellvorstellungen zur Verbreitung potentieller präwestfalischer Erdgas-Muttergesteine in Norddeutschland – Ergebnisse neuer magnetotelurischer Messungen. Zeitschrift für Angewandte Geologie 44 (3): 140-158.

IES *(Integrated Exploration System) PetroMod Manuals Release 5.0, Part 7:* Theoretical Aspects-PetroGen/PetroFlow.

Koch, J. & Arnemann, H., 1975. Die Inkohlung der Gesteine des Rhät und Lias im südlichen NW-Deutschland. Geologisches Jahrbuch A 29: 45-55.

Kockel, F., 1998. Geotektonischer Atlas von Nordwestdeutschland (1:300000) Teil 18: Die Paläogeographie und strukturelle Entwicklung Nordwestdeutschlands. Band 3, BGR, (unpublished report), Nr.: 00400802.

Kockel, F., 2002. Rifting processes in NW-Germany and the German North Sea Sector. Netherlands Journal of Geosciences 8 (2): 149-158.

Kockel, F. & Franzke, H.J., 1998. Excursion guide. The Subhercynian Region, the Northern Harz boundary. Leipziger Geowissenschaften 7: 45-71.

Kockel, F., Wehner, H. & Gerling, P., 1994. Petroleum systems of the Lower Saxony basin, Germany. *In:* Magoon & Dow (eds): The petroleum system – from source to trap. AAPG Memoire 60: 573-586.

Kockel, F., Brückner-Röhling, S., Röhling, H.-G. & Frisch, U., 1999. Geotektonischer Atlas von Nordwestdeutschland 1:300000; Teil 18 Die paläographische und strukturelle Entwicklung Nordwestdeutschlands; Band 1, BGR, (unpublished report), Nr.: 00400791.

Krooss, B. M., Leythaeuser, D. & Lillack, H., 1993. Nitrogen rich Natural Gases. – Qualitative and Quantitative Aspects of Natural Gas Accumulations in Reservoirs. Erdöl Kohle-Erdgas-Petrochemie 46: 271-276.

Lachenbruch, A. & Brewer M., Dissipation of the temperature effect of drilling a well in arctic Alaska, 1959. Geological. Survey Bulletin, 1083-C: 73-109.

Leblanc, Y., H.-L. Lam, Pascoe, L. J. & F. W. Jones, 1982. A comparison of two methods of estimating static formation temperature from well logs, Geophys. Prospect., 30: 348-357.

Leischner, K., 1994. Kalibration simulierter Temperaturgeschichten von Sedimentgesteinen. Inst. für Chemie und Dynamik der Geosphäre 4, Erdöl und organische Geochemie. Berichte. des Forschungszentrums Jülich, 2909: 1-309.

Littke, R., Leythaeuser, D., Radke, M. & Schaefer, R.G., 1990. Petroleum generation and migration in coal seams of the Carboniferous Ruhr Basin, Northwest Germany. *In:* Durand, B. and Behar, F. (eds): Advanced. Organic Geochemistry 16: 247-258.

Lokhorst, A., Adlam, K., Brugge, J.V.M., David, P., Diapari, L., Fermont, W.J.J., Geluk, M., Gerling, P., Heckers, J., Kockel, F., Kotarba, M., Laier, T., Lott, G.K., Milaczewski, E., Milaczewski, L, Nicholson, R.A., Platen, F.V. & Pokorski, J., 1998. NW European Gas Atlas – Composition and Isotope Ratios of Natural Gases. – CD ROM (ISBN: 90-72869-60-5).

Menning, M., Davydov, V., Drozdzewski, G., Wendt, I. & Weyer, D., 1997. Kalibrierung der Zeitskalen von Karbon und Perm: in Kolloquium 1: Stratigraphie, Sedimentation und Beckenentwicklung im Karbon und Perm: 29-30.

Neugebauer, H.J. & Reuther, C., 1987. Intrusion of igneous rocks – physical aspects. Geologischer Rundschau 76: 89-99.

Nodop, I., 1971. Tiefenrefraktionsseismischer Befund im Profil Versmold. Lübecke-Nienburg. Fortschritte in der Geologie von Rheinland und Westfalen 18: 411-422.

Pavlenkova, N.I., 1995. Structural regularities in the lithosphere of continents and plate tectonics. Tectonophysics, 243, 223-229.

Pavlenkova, N.I., 1998. Endogenous regimes and plate tectonics in northern Eurasia. Physics and Chemistry of the Earth, 23, 799-810.

Pasternak, M., Brinkmann, S., Messner, J. & Sedlacek, R., 2003. Erdöl und Erdgas in der Bundesrepublik Deutschland 2002. NLfB, (unpublished report), Nr.: 00816104.

Patniak, P. & Füchtbauer, H., 1975. Temperature influencing the authigenetic growth of silicates. IXth International Congress of Sedimentology, Nice. Theme 7: 163-168.

Petmecky, S., Meier, L., Reiser, H. & Littke, R., 1999. High thermal maturity in the Lower Saxony basin: intrusion or deep burial? Tectonophysics 304: 317-344.

Plaumann, S., 1983. Die Schwerekarte 1:500 000 der Bundesrepublik Deutschland (Bouger-Anomalien), Blatt Nord. Geologisches Jahrbuch E 27: 1-16.

Plaumann, S., 1991. Die Schwerekarte 1:500 000 der Bundesrepublik Deutschland (Bouger-Anomalien), Blatt Nord. Geologisches Jahrbuch. E 46: 1-16.

Pratt, D., 2000. Plate Tectonics: a paradigm under threat. Journal of scientific exploration 14(3): 307-352.

Reich, H., 1933. Erdmagnetismus und saxonische Tektonik. Zeitschrift der Deutschen Geologischen Gesellschaft 85: 635-646.

Richter, D. K., Bruckschen, P. & Kharti, S., 1986. Zur hochdiagenetischen Beeinflussung der Mikrodolomite im Trochitenkalk (mo1) durch die Massivreihe Bramsche-Vlotho-Solling. *In:* Bechstädt, T. & Knieter, H (Hrsg.): Erstes Treffen deutschsprachiger Sedimentologen. Universität Freiburg: 1: 93-96.

Scheidt, G. & Littke, R., 1989. Comparative organic petrology of interlayered sandstones, siltstones, mudstones and coals in the Upper Carboniferous Ruhr basin, Northwest Germany, and their thermal history and methane generation. Geologischer Rundschau 78 (1): 375 – 390.

Schmidt-Mumm, A., 1995. Mikrothermische Untersuchungen an Flüssigkeiten insbesondere Diageneseminералien der Bohrungen Anaveen-Z1, Dustmoor-Z1, Apeldorn-Z2, Schale-Z1, Menslage-Z1. BGR, (unpublished report), Nr.: 0115151.

Schmitz, H.-H., 1968. Untersuchungen am nordwestdeutschen Posidonienschiefer und seiner organischen Substanz. Beihefte des Geologischen Jahrbuchs 58: 1-220.

Schmitz, U., 1990. The Relation of Thermogradient Distribution and Regional Geology in NW Germany, particularly in the Bramsche-Vlotho Massif Area. Erdöl, Erdgas, Kohle 106 (5): 189-193.

Schmitz, U. & Wenzlow, B., 1991. Maturity anomalies of the western Saxony Basin in their regional geological context. Zentralblatt für Geologie und Paläontologie I, 8: 1091-1103.

Schreyer, D., 1968. Lagerstättenkundliche Untersuchungen an hydrothermalen Vererzungen im Osnabrücker Raum. Univ. Münster, Unpublished PhD Thesis: 150 pp.

Schreyer, D., 1969. Zum Vorkommen von Pyrophyllit, Gümbelit und Quarziten in der Kontaktaureole des Bramscher Massivs. Geologischer Rundschau 80: 83-977.

Senglaub, Y., Littke, R. & Brix, M.R., 2004. Burial and temperature history in the area of the Bramsche anomaly, Lower Saxony Basin – Schriftenreihe der Deutschen Geologischen Gesellschaft, 33: 146.

Sneider, R., Surdam, R. & Vavra, Ch., 2000. Seals – a critical element to successful exploration and production. PTTC' Eastern Golf Region, Jackson, Mississippi, 29.03.2000.

Stadler, G., 1971. Die Vererzung im Bereich des Bramscher Massivs und seiner Umgebung. Fortschritte in der Geologie von Rheinland und Westfalen 18: 439-500.

Stadler, G. & Teichmüller, R., 1971. Zusammenfassender Überblick über die Entwicklung des Bramscher Massivs und des Niedersächsischen Tektogens. Fortschritte in der Geologie von Rheinland und Westfalen 18: 547-564.

Stadler, G. & Teichmüller, R., 1982. Kontaktmetamorphe Valendis-Sandsteine bei Sulingen am Nordrand des Niedersächsischen Beckens und ihre Bedeutung für das Alter der Erdölmigration. Neues Jahrbuch für Geologie und Palaeontologie 1: 50-63.

Strohmenger, C., Antonini, M., Jäger, G., Rockenbauch, K. & Strauss, C., 1996. Zechstein 2 carbonate reservoir facies distribution in relation to Zechstein sequence stratigraphy (Upper Permian, Germany): an intergrated approach. Bulletin des centres de recherché exploration-production Elf-Aquitaine 20 (1): 1-35.

Sweeney, J.J. & Burnham, A.K., 1990. Evaluation of a simple model of vitrinite reflectance based on chemical kinetics. AAPG Bulletin 74: 1559-1570.

Teichmüller, M., Teichmüller, R. & Bartenstein H., 1984. Inkohlung und Erdgas - eine neue Inkohlungskarte der Karbon-Oberfläche in Nordwestdeutschland. Fortschritte in der Geologie von Rheinland und Westfalen 32: 11-34.

Teichmüller, M. & Teichmüller, R., 1950. Das Inkohlungsbild des Niedersächsischen Wealdenbeckens. Zeitschrift der Deutschen Geologischen Gesellschaft 100: 498-517.

https://doi.org/10.1017/S0016774600022873 Published online by Cambridge University Press

Teichmüller, M. & Teichmüller, R., 1951. Inkohlungsfragen im Osnabrücker Raum. Neues Jahrbuch für Geologie und Palaeontologie 1951: 69-85.

Teichmüller, M. & Teichmüller, R., 1971. Inkohlung. *In:* Die Karbonablagerungen in der Bundesrepublik Deutschland. Fortschritte in der Geologie von Rheinland und Westfalen 19: 69-72.

Teichmüller, M., Teichmüller, R. & Bartenstein, H., 1979. Inkohlung und Erdgas in Nordwestdeutschland. Eine Inkohlungskarte der Oberfläche des Oberkarbons. Fortschritte in der Geologie von Rheinland und Westfalen 27: 137-170.

Teichmüller, R. & Teichmüller, M., 1985. Inkohlungsgradienten in der Anthrazitfolge des Ibbenbürener Karbon. Fortschritte in der Geologie von Rheinland und Westfalen 33: 231-253.

Tischendorf, G., 1987. Probleme des Magmatismus und seiner Metallogenese im variszisch konsolidierten Mitteleuropa. Zeitschrift für geologische Wissenschaften 15 (1): 5-23.

Thyssen, F., Allnoch, G. & Lütkebohmert, G., 1971. Einige Ergebnisse geophysikalischer Arbeiten im Bereich der Bramscher Anomalie. Fortschritte in der Geologie von Rheinland und Westfalen 18: 395-410.

TNO-NITG, 2001. Information 2000, http://www2.tnodiana.com/gs/rdas/pages/html/pdfcs/3d_model_gas_field.pdf

Voigt, E., 1962a. Über Randtröge vor Schollenrändern und ihre Bedeutung im Gebiet der Mitteleuropäischen Senke und angrenzender Gebiete. Zeitschrift der Deutschen Geologischen Gesellschaft 114 (2): 378-418.

Voigt, E., 1962b. Frühdiagenetische Deformation der Turonen Plänerkalke bei Halle/Westfalen als Folge einer Großgleitung unter besonderer Berücksichtigung des Phakoid-Problems. Mitteilungen des Geologischen Staatsinstitutes 31: 146-275.

Wohlenberg, J., 1979. The subsurface Temperature Field of the Federal Republic of Germany. Geologisches Jahrbuch E 15: 3-29.

Wehner, H., Binot, F., Gerling, P., Hiltmann, W. & Kockel, F., 1989. Genese und Migration von Erdölen im Niedersächsischen Becken, Abschlußbericht für das westliche Niedersächsiche Becken. BGR, (unpublished report) Nr.:106 255.

Wonham, J. P., Johnson, H.D., Mutterlose, J., Stadler, A. & Ruffell, A., 1997. Characterisation of a shallow marine sandstone reservoir in a syn-rift setting: the Bentheimer Sandstone Formation (Valanginian) of the Rühlermoor field, Lower Saxony Basin, NW Germany. *In:* Shanley & Perkins (eds): Shallow marine and non-marine Reservoirs: Sequence stratigraphy, reservoir architecture and production characteristics. Society of Economic Paleontologists and Mineralogists., Gulf Coast Sect. 18th Ann. Res. Conference: 427-448.

Ziegler, P.A., 1987a. Late Cretaceous and Cenozoic intra-plate deformations in the Alpine foreland- a geodynamic model. Tectonophysics 137: 389-420.

Ziegler, P.A., 1987b. Compressional intra-plate deformations in the Alpine foreland. Tectonophysics 137: 1-420.

Ziegler, P.A., Cloetingh, S. & Van Wees, J.-D., 1995. Dynamics of intra-plate compressional deformation: the Alpine foreland and other examples. Tectonophysics 252: 7-59.

Ziegler, P.A., 1998: Collisional intraplate deformation. GFF, Vol. 120 (Pt. 2, June), pp. 249-256.